Supporting Information

The Temperature Dependence of C-H...F-C Interactions in Benzene:Hexafluorobenzene

Jeremy K. Cockcroft, Alexander Rosu-Finsen, Andrew N. Fitch and Jeffrey H. Williams

Table of Contents Page No.

Additional Experimental Details

1. Sample Preparation. 3

2. PXRD Measurements and Analysis. 3

3. DSC Measurements and Analysis. 5

4. SXD Measurements and Analysis. 6

List of Tables

SXD data on phase I of C_6H_6:C_6F_6.

Table S1a. Crystal data and structure refinement. 8

Table S1b. Fractional atomic coordinates and U(eq) for all atoms. 8

Table S1c. Anisotropic displacement parameters. 9

SXD data on phase II of C_6H_6:C_6F_6.

Table S2a. Crystal data and structure refinement. 10

Table S2b. Fractional atomic coordinates and U(eq) for all atoms. 10

Table S2c. Anisotropic displacement parameters. 11

PND-PXRD data on phase III of C_6D_6:C_6F_6.

Table S3a. Crystal data and structure refinement. 12

Table S3b. Fractional atomic coordinates and U(eq) for all atoms. 12

Table S3c. Anisotropic displacement parameters. 13

Variable temperature PND data on C_6D_6:C_6F_6.

Table S4a. Lattice parameters for phase IV on heating. 14

Table S4b. Lattice parameters for phase III on heating. 18

Table S4c. Lattice parameters for phase II on heating. 19

Table S4d. Lattice parameters for phase I on heating. 20

Table S4e. Lattice parameters for phase I on cooling. 21

Table S4f. Lattice parameters for phase II on cooling. 22

Table S4g. Lattice parameters for phase III on cooling. 23

List of Figures

Fig. S1. PND data of C_6D_6:C_6F_6 measured on D1B. 27

Fig. S2. Lattice parameters of C_6D_6:C_6F_6 on heating/cooling from D1B data. 28

Fig. S3. Laboratory PXRD data of C_6F_6:C_6H_6 from 100 K to 290 K. 29

Fig. S4. PND data of C_6D_6:C_6F_6 measured on D1A. 30

Fig. S5. DSC data for C_6H_6 (upper) and C_6F_6 (lower). 31

Fig. S6. Single-crystal of C_6H_6:C_6F_6 measured on Agilent SuperNova. 32

Fig. S7. Atomic labelling scheme used for C_6H_6:C_6F_6 phases I to IV. 33

Fig. S8. Rietveld refinement fit to PND data of C_6F_6:C_6D_6 phase IV. 34

Fig. S9. Bond-dipole interactions in C_6H_6:C_6F_6 phase IV (plane). 35

Fig. S10. Bond-dipole interactions in C_6H_6:C_6F_6 phase IV (sheets). 36
Fig. S11. Rietveld fit to neutron data of C_6F_6:C_6D_6 phase III using sub-cell. 37
Fig. S12. View of the initial crystal structure of C_6H_6:C_6F_6 phase III. 38
Fig. S13. LeBail fits to PXRD synchrotron data of C_6F_6:C_6H_6 phase III. 39
Fig. S14. Combined Rietveld refinement fit to C_6F_6:$C_6D(H)_6$ phase III. 40
Fig. S15. Bond-dipole interactions in C_6H_6:C_6F_6 phase III (plane). 41
Fig. S16. Bond-dipole interactions in C_6H_6:C_6F_6 phase III (sheets). 42
Fig. S17. Bond-dipole interactions in C_6H_6:C_6F_6 phase III (oblique view). 43
Fig. S18. LeBail fit to PXRD synchrotron data of C_6F_6:C_6H_6 phase II. 44
Fig. S19. Rietveld refinement fit to PND data of C_6F_6:C_6D_6 phase II. 45
Fig. S20. Electron density map showing disorder of C_6H_6 in phase II. 46
Fig. S21. Rietveld refinement fit to PND data of C_6F_6:C_6D_6 phase I. 47
Fig. S22. Raw SXD data frames of C_6F_6:C_6H_6 phase I showing TDS. 48
Fig. S23. Electron density map showing localised position for C_6F_6 in phase I. 49

Additional Experimental Details

1. Sample Preparation

For the powder neutron diffraction experiments in 1990 and 1991, approx. 10 cm^3 of C_6D_6:C_6F_6 was prepared by addition of the isolated components in a 1:1 molar ratio. Deuterated benzene (> 99% D) was used in order to avoid the large incoherent scattering from H atoms in hydrogenated benzene. For the synchrotron X-ray radiation powder diffraction experiments in 1991, a sample was prepared using protonated benzene, C_6H_6.

For the laboratory powder and single-crystal X-ray diffraction and DSC experiments in 2017, $^1/_{100}$ mole of sample was prepared by the addition of 0.784 g of benzene (Sigma-Aldrich, 27,070-9, 1 L, MW=78.11, HPLC grade > 99.9%) and 1.861 g of hexafluorobenzene (Aldrich H8706, 100 g, MW=186.05, 99%) in a small sealable bottle. The sealed bottle was gently heated in warm water (40-50 °C) to dissolve the solid and ensure complete mixing of the liquid components and then left in a fridge (5 °C) to solidify and to minimise loss of either one or both components.

2. Powder Diffraction Measurements and Analyses

The large sample of C_6D_6:C_6F_6 was ground N_2 under in a ceramic mortar standing in liquid N_2 in a polystyrene box and filled into a thin-walled cylindrical vanadium sample holder (50 mm × 16 mm Ø). The sample was transferred to a liquid He cryostat pre-cooled to 10 K. Measurements were made continuously over a 24 hour period on the diffractometer D1B at the ILL with diffraction patterns being saved each minute. Over this period, the temperature of the sample was ramped from 10 K to 290 K at 1 K min^{-1} (data shown in Fig. 1), held at 290 K, then cooled back to 100 K at 0.4 K min^{-1} before finally heating back to 290 K at the same ramp rate as shown in Fig. S1.

High-resolution powder neutron diffraction patterns appropriate for indexing were collected on D1A with λ = 2.99 Å (nominal) with the sample at 1.5 K (phase IV), 150 K (IV), 225 K (III), 260 K (II) and 285 K (I). Each scan was made in approx. 6 hours. The quality of the data is seen in Fig. S4. Data sets obtained for Rietveld refinement (6° to 156° in steps of 0.05° 2θ) were measured with a nominal wavelength λ = 1.9087 Å at 1.5 K (phase IV) and 225 K (III) in 13 and 22 hours, respectively.

Synchrotron powder X-ray diffraction data were collected on the diffractometer 2.3 at the Daresbury Laboratory with λ = 1.40302(2) Å using a liquid helium cryostat and a flat-plate sample holder. Measurements were made at samples temperatures 30 K (5° to 117° in steps of 0.01° 2θ), 215 K (5° to 85°), and 260 K (5° to 80°).

For comparison with the neutron diffraction data, laboratory powder X-ray diffraction data were collected of a sample of C_6H_6:C_6F_6 in a spinning 1 mm capillary using a Stoe Stadi-P® diffractometer equipped with a Cu anode, Ge<111> monochromator, a Dectris Mythen 1K® detector, and an Oxford Instruments CryojetHT® (90-500 K) with an in-house modified sample setup and software. The sample was cooled to 100 K and measurements were made on heating in 10 K intervals to 300 K (Fig. S3). The detector was scanned in 2θ from 5° to

50° in steps of 0.5° at 15 s per step, a complete scan lasting approx. 30 min; each 10 K temperature ramp took about 10 min and the sample was equilibrated for a further 5 min.

Lattice parameters were obtained from the D1B data as a function of temperature (shown in Fig. 5 and Fig. S2) using a structure-constrained Rietveld refinement using the program PROFIL v7.02 for phases IV-II. Given the course wire spacing of the instrument (0.2° step in 2θ), conventional Pawley or LeBail whole-pattern fitting methods could not be used to determine the lattice parameters as false minima were frequently obtained. Hence the data could not be fitted over the whole temperature range until the structure of each of the phases II, III, and IV were solved. For phase IV, a total of 13 parameters were used (scale factor, 4 lattice parameters and the 2θ zero, 4 peak width and shape parameters, and overall isotropic *B*-values for C, F, and D with atomic coordinates constrained as per the structure solution at 1.5 K.) For phase III and II which exist over increasingly narrower temperature ranges, fewer parameters were required. For phase I where there are fewer problems with false minima, LeBail whole pattern fitting was used to refine the cell parameters from the data, but with the unit cell halved along **c** due to the very similar scattering of dynamically-disordered C_6D_6 and C_6F_6. Diffraction patterns exhibiting two phases in coexistence were omitted from the fitting procedure. A table of refined values is provided in Table S1. The volume change per dimer as a function of temperature is shown in Fig. 4. The rates of change of the individual lattice parameters (on both heating and cooling) are seen in Fig. S2. Lattice parameters of the 4 phases were also determined using the same method as above from D1A data measured with $\lambda = 2.99$ Å, and values are given in Table 1.

The crystal structures of phases IV and III were determined from both synchrotron X-ray radiation and neutron powder diffraction data sets. The structure of phase IV was previously published in reference[1]. In summary, the structure was solved from the synchrotron data set of the sample at 30 K using the direct methods program SIR88.[2] The structure was refined from the D1A data with $\lambda = 1.9087$ Å of the sample at 1.5 K (Fig. S8). The structure was re-fitted to the original data and the numbers presented here for phase IV are in good agreement with those published previously.

A preliminary unpublished structure of phase III was presented orally at the IUCR XVI congress in Beijing, 1993.[3] As for phase IV, the unit of phase III was determined from the high-resolution synchrotron PXRD data from 2.3 but conventional single-crystal methods were unable to solve the more complex triclinic structure in contrast to the success obtained with the data from monoclinic phase IV. The solution was to use all of the information available from X-ray data, neutron data, and chemical insight. Although the structure is primitive triclinic, around 95% of the peak intensity in the neutron data set could be accounted for in terms of a *C*-face centred triclinic cell with the *c*-axis halved to about 3.6 Å due to the similar scattering of C_6D_6 and C_6F_6 with neutrons (see Fig. S11 and Fig. S12). In phase IV, the inter-ring spacing along the *c*-axis has a similar value. This suggested that the rings are stacked along the *c*-axis in phase III with parallel faces with the same orientation, i.e. with C above C and F above D. Using the neutron data and the sub-cell, the orientation of a single average C_6F_6/C_6D_6 ring can be found by Rietveld refinement analysis in space group

[1] J. H. Williams, J. K. Cockcroft and A. N. Fitch, *Angew. Chem., Int. Ed. Engl.*, 1992, 31, 1655–1657.
[2] M. C. Burla, M. Camalli, G. Cascarano, C. Giacovazzo, G. Polidori, R. Spagna and D. Viterbo, *J. Appl. Crystallogr.*, 1989, **22**, 389–393.
[3] J. K. Cockcroft, A. N. Fitch and J. H. Williams, *Acta Crystallogr.*, 1993, **A49** suppl. C24.

$C\bar{1}$. With the unit cell then doubled along *c*-axis to about 7.2 Å, most of the intensity in the X-ray data can be accounted for in terms of a pseudo *I*-centred triclinic cell (Fig. S13). That the correct structure is primitive is evident from the observation of a relatively strong $\bar{1}02$ reflection. However, an unconstrained Rietveld refinement would require 216 structural parameters which is not viable even with combined data of this quality. The large number of parameters may be reduced by imposing 6/*m* point symmetry on each ring and by using a TLS model of thermal libration (with S set to zero) to constrain the thermal ellipsoid of each atom. The parameters from the best fit based on a Rietveld refinement with combined synchrotron X-ray and neutron data sets (Fig. S14) are given in Table S3. Views of the crystal structure of phase III are shown in Fig. S15-17. The mean bond lengths from the refined coordinates are: in C_6F_6, C–C and C–F are equal to 1.395 Å and 1.404 Å, respectively, and in C_6D_6, C–C and C–D are equal to 1.404 Å and 1.003 Å, respectively.

The unit cell of phase II was initially determined from the synchrotron X-ray diffraction data set of the sample measured at 260 K.[1] The LeBail fit to the data shown in Fig. S18 demonstrates the lack of any measureable Bragg peak intensity in the PXRD pattern above the 1.5 Å resolution limit. The latter was a strong influencing factor in the choice of frames for the SXD measurements reported here for both phases I and II. Once the structure of phase II had been solved from the SXD data, a Rietveld refinement was performed using the original high-resolution diffraction measured on D1A with $\lambda = 2.99$ Å as a check for consistency between X-ray and neutron measurements. The single-crystal model from SXD is in good agreement with the neutron data. (Fig. S19). Likewise, once a satisfactory model was obtained from the SXD data for phase I, a similar Rietveld refinement was made against the original neutron data from D1A with $\lambda = 2.99$ Å measured on the deuterated sample at 285 K.

3. DSC Measurements

18.52 mg of C_6H_6:C_6F_6 was loaded into a steel sample pan using a Mettler 5 digit balance. The sample pan was quickly sealed with a screw lid and then loaded into PerkinElmer DSC8000 calorimeter at +20 °C. A helium purge gas was used for all experiments (40 mL min^{-1}). As a result of the hysteresis observed previously in powder diffraction experiments, a scan sequence was employed which involved cycling between phases III and IV in addition to a standard sequence of cooling from phase I and heating back to the melt. Prior to each heating cooling or heating ramps at 10 °C min^{-1}, the sample was held isothermally for 1 min. The sample was initially cooled to −150 °C, heated to −30 °C, cooled to −150 °C, heated to −30 °C, and then cooled back again to −150 °C. The next heating cycle took the sample to phase I at 15 °C, followed by a cooling cycle to −150 °C, and finally heating back to 30 °C (the onset of melting).

The heating cycle from −150 °C to 15 °C was highly reproducible when the previous cooling cycle started from the sample in phase I. Typical data is shown in Fig. 2. Likewise, cooling from 10 °C to −90 °C resulted in highly reproducible data, but subsequent data on further cooling to phase IV resulted in erratic heat flow, probably due to different crystallites transforming to phase IV at different temperatures, consistent with the hysteresis observed in powder diffraction experiments. Subsequent thermal cycling between −30 °C (phase III) and −150 °C (a mixture of phases III and IV) indicates that the degree of transformation from

phase III to phase IV is reduced after the initial cooling cycle from phase I. On heating, broad transitions are observed at 222.3(3) K (ΔH = 1.3(1) kJ mol^{-1}) and 256.5(3) K (ΔH = 0.65(5) kJ mol^{-1}) corresponding to transitions from phase IV to phase III and from phase III to phase II, respectively. Assuming that only half of the sample transforms to phase IV on cooling, the enthalpy for the phase IV to phase III transition must be much larger, and is probably around 2 to 3 kJ mol^{-1}. The final transition observed on heating is due to an overlap of the transition from phase II to phase I plus the melting of the eutectics of benzene and hexafluorobenzene. By contrast, the reverse transition from phase I to phase II can be seen more clearly on cooling in Fig. 2 as it is separated from the eutectic transitions in temperature: the transition temperature is 264.6(3) K (ΔH = −0.05(1) kJ mol^{-1}).

Two control DSC experiments were performed on the individual components: the masses of C_6H_6 and C_6F_6 used were 18.15 mg and 21.65 mg, respectively. For these samples a simple scan strategy was performed: the sample was cooled at 10 °C min^{-1} from 20°C to −150°C, held for 1 min, and then heated at 10 °C min^{-1} to 25°C. The data are shown in Fig. S5. Each sample was observed to freeze sharply (+5.18 °C and −0.38 °C for C_6H_6 and C_6F_6, respectively) and the enthalpies of fusion (ΔH = 10.0 kJ mol^{-1} and 11.6 kJ mol^{-1}) are in excellent agreement with literature values.[4] All values were determined using the Pyris software package (version 11.1.1.0492) from PerkinElmer.

4. SXD Measurements and Analysis

The binary adduct was melted by heating the sealed bottle in warm water (40-50 °C) and a small amount of liquid was pipetted into the neck of a 0.5 mm X-ray capillary held in the same warm water. The liquid was shaken to the end of the capillary, which was subsequently flame sealed (Fig. S6). A full sphere of diffraction data was collected for phase I at 280 K to a resolution of d_{min} = 1.5 Å. On cooling slowly to 260 K, the crystal fragmented into several pieces. Despite the fragmentation, the data were processed in terms of 4 independent crystals with the CrysAlisPro software package (version 1.171.38.43) from Rigaku Oxford Diffraction.

The structure of phase II was solved in space group *I*2/*m* and refined by least-squares within the Olex2 program suite[5] using the ShelXT structure solution program and the ShelXL 2014 refinement program[6]. The hydrogen atoms on the C_6H_6 ring were constrained with the ShelXL AFIX 43 instruction. To avoid false minima, a thermal motion restraint (SIMU) was also applied. A Fourier electron density map based on F_{obs} (with phases from $\mathbf{F}_{calc}$) demonstrates that at this temperature, and on the time scale of the measurement, the C_6H_6 rings are losing their distinct hexagonal symmetry and are becoming toroidal, which is not the case for the C_6F_6 molecules at this temperature (Fig. S20). The bond lengths derived from the refined coordinates (C1–C1 = 1.34(4) Å, C1–C2 = 1.37(2) Å, C1–F1 = 1.338(16) Å, and C1–

[4] O. Maass and L. J. Waldbauer, *J. Am. Chem. Soc.*, 1925, **47**, 1-9; J. F. Messerly and L. Finke. *J. Chem. Thermodyn.*, 1970, **2**, 867–880.
[5] O. V. Dolomanov, L. J. Bourhis, R. J. Gildea, J. A. K. Howard and H. Puschmann, *J. Appl. Crystallogr.*, 2009, **42**, 339-341.
[6] G. M. Sheldrick, *Acta Crystallogr.*, 2015, **C71**, 3–8.

F2 = 1.30(3) Å in C_6F_6 and C3–C3 = 1.30(2) Å, C3–C4 = 1.367(13) Å, and all C–H fixed at 0.93 Å in C_6H_6) are shortened due to thermal motion.

The evolution of the molecular motion in the adduct is evident in the raw diffraction data, particularly at the higher temperatures where thermal diffuse scattering is readily seen for both phases I and II (*e.g.* as seen in Fig S22). The structure of phase I was solved by simple model building in space group $R\bar{3}m$ (as used in a previous inconclusive attempt to describe the structure[7]) and refined to a satisfactorily low *R*-factor. The plane of the rings was assumed to be perpendicular to the threefold axis with C_6F_6 centred at 0,0,0 and C_6H_6 centred at 0,0,½. Given the high symmetry, the number of unique reflections is low and false minima are all too easily obtained in the least-squares refinement, so a CGLS minimisation was used using ShelXL[6] from within Olex2[5]. A Fourier electron-density map based on F_{obs} (with phases from $\mathbf{F}_{calc}$) still shows distinct positions for C_6F_6 consistent with a molecule undergoing thermally-driven jump rotations (Fig. S23), but a well-developed torus is seen in the map for C_6H_6 consistent with a molecule undergoing free or near free rotation — in the limit of the jump rotation model. The torus is best modelled using C-atoms with large ellipsoids but with the H-atom electron density split 50:50 with an isotropic *B* value tied to the C-atoms. In addition, a distance restraint was applied so that the H atoms lay on a common circumference around the C atoms (as seen in Fig. 3). The bond lengths derived from the refined coordinates (C1–C1 = 1.340(13) Å, C1–F1 = 1.324(9) Å, and C2–C2 = 1.27(6) Å) are significantly shortened due to thermal motion.

[7] J. S. W. Overell and G. S. Pawley, *Acta Crystallogr.*, 1982, **B38**, 1966–1972.

Table S1a. Crystal data and structure refinement for phase I of C_6H_6:C_6F_6.

Identification code	exp_1040
Empirical formula	$C_{12}H_6F_6$
Formula weight	264.18
Temperature / K	280
Crystal system	trigonal
Space group	$R\bar{3}m$
a / Å	11.9880(14)
b / Å	11.9880(14)
c / Å	7.2416(10)
α / °	90
β / °	90
γ / °	120
Volume / Å^3	901.3(2)
Z	3
ρ_{calc} / g cm^{-3}	1.460
μ / mm^{-1}	1.355
F(000)	396.0
Crystal size / mm^3	0.916 × 0.404 × 0.371
Radiation	CuKα (λ = 1.54184)
2θ range for data collection / °	14.916 to 60.398
Index ranges	$-7 \le h \le 7$, $-7 \le k \le 7$, $-4 \le l \le 4$
Reflections collected	497
Independent reflections	38 [R_{int} = 0.0517, R_{sigma} = 0.0137]
Data/restraints/parameters	38/1/18
Goodness-of-fit on F^2	1.397
Final R indexes [I >= 2σ(I)]	R_1 = 0.0402, wR_2 = 0.0720
Final R indexes [all data]	R_1 = 0.0407, wR_2 = 0.0721
Largest diff. peak/hole / e Å^{-3}	0.07/−0.04

Table S1b. Fractional atomic coordinates and equivalent isotropic displacement parameters (Å^2) for phase I of C_6H_6:C_6F_6. U_{eq} is defined as ⅓ of the trace of the orthogonalised U_{ij} tensor.

Atom	*x*	*y*	*z*	*U*(eq)
F(1)	0	0.2222(6)	0	0.288(6)
C(1)	0	0.1118(11)	0	0.193(8)
C(2)	0.059(3)	0.118(5)	0.5000	0.34(6)
H(2A)	0.102(3)	0.204(7)	0.5000	0.412
H(2B)	0	0.178(6)	½	0.412

Table S1c. Anisotropic displacement parameters (Å^2) for phase I of C_6H_6:C_6F_6. Anisotropic displacement factor exponent has the form: $-2\pi^2[h^2a^{*2}U_{11}+2hka^*b^*U_{12}+\ldots]$.

Atom	U_{11}	U_{22}	U_{33}	U_{23}	U_{13}	U_{12}
F(1)	0.372(10)	0.230(6)	0.310(9)	0.000(3)	0.001(6)	0.186(5)
C(1)	0.250(20)	0.191(8)	0.156(8)	0.000(3)	0.000(5)	0.127(10)
C(2)	0.56(13)	0.182(19)	0.164(7)	−0.007(9)	−0.003(4)	0.091(10)

Table S2a. Crystal data and structure refinement for phase II of C_6H_6:C_6F_6.

Identification code	exp_1042_twin3_hklf4
Empirical formula	$C_{12}H_6F_6$
Formula weight	264.17
Temperature / K	260
Crystal system	monoclinic
Space group	$I2/m$
a / Å	6.6707(18)
b / Å	12.315(2)
c / Å	7.305(2)
α / °	90
β / °	100.14(2)
γ / °	90
Volume / Å^3	590.7(3)
Z	2
ρ_{calc} / g cm^{-3}	1.485
μ / mm^{-1}	1.378
F(000)	264.0
Crystal size / mm^3	0.859 × 0.448 × 0.402
Radiation	CuKα (λ = 1.54184)
2θ range for data collection / °	14.262 to 62.272
Index ranges	$-4 \le h \le 4$, $-7 \le k \le 8$, $-4 \le l \le 4$
Reflections collected	467
Independent reflections	98 [R_{int} = 0.0567, R_{sigma} = 0.0354]
Data/restraints/parameters	98/24/43
Goodness-of-fit on F^2	1.178
Final R indexes [I >= 2σ(I)]	R_1 = 0.0521, wR_2 = 0.1115
Final R indexes [all data]	R_1 = 0.0546, wR_2 = 0.1157
Largest diff. peak/hole / e Å^{-3}	0.11/−0.19

Table S2b. Fractional atomic coordinates and equivalent isotropic displacement parameters (Å^2) for phase II of C_6H_6:C_6F_6. U_{eq} is defined as ⅓ of the trace of the orthogonalised U_{ij} tensor.

Atom	x	y	z	U(eq)
F(1)	0.3436(13)	0.1091(7)	0.1347(8)	0.233(4)
F(2)	0	0.2173(10)	0	0.244(6)
C(1)	0.174(3)	0.0544(14)	0.0655(14)	0.137(5)
C(2)	0	0.112(3)	0	0.154(9)
C(3)	0.1744(14)	0.0527(9)	0.5578(12)	0.170(7)
C(4)	0	0.1106(17)	½	0.173(7)
H(3)	0.2958	0.0896	0.5980	0.204
H(4)	0	0.1861	½	0.208

Table S1c. Anisotropic displacement parameters (Å^2) for phase II of C_6H_6:C_6F_6. Anisotropic displacement factor exponent has the form: $-2\pi^2[h^2a^{*2}U_{11}+2hka^*b^*U_{12}+\ldots]$.

Atom	U_{11}	U_{22}	U_{33}	U_{23}	U_{13}	U_{12}
F(1)	0.162(7)	0.318(10)	0.209(6)	−0.035(4)	0.006(5)	−0.090(5)
F(2)	0.296(11)	0.170(11)	0.264(9)	0	0.049(6)	0
C(1)	0.13(2)	0.16(3)	0.122(8)	−0.018(6)	0.023(10)	−0.029(11)
C(2)	0.18(4)	0.15(4)	0.140(14)	0	0.050(18)	0
C(3)	0.141(12)	0.22(2)	0.145(8)	−0.005(7)	0.014(6)	−0.023(7)
C(4)	0.22(3)	0.14(2)	0.158(14)	0	0.035(15)	0

Table S3a. Crystal data and structure refinement using the Rietveld method for phase III of C_6D_6:C_6F_6 from combined powder synchrotron X-ray and neutron diffraction data. Further details are given above in Section 2.

Identification code	PXRD_and_PND_phaseIII
Empirical formula	$C_{12}D_6F_6$
Formula weight	540.24
Temperature / K	220
Crystal system	triclinic
Space group	$P\bar{1}$
a / Å	6.38014(12)
b / Å	12.3380(3)
c / Å	7.29433(10)
α / °	93.9904(12)
β / °	96.7395(10)
γ / °	91.8409(14)
Volume / Å^3	568.38(3)
Z	2
ρ_{calc} / g cm^{-3}	1.578
Radiation	X-ray (λ = 1.40302)
Radiation	neutron (λ = 1.90818(15))
2θ range for X-ray data / °	5.0 to 74.99
2θ range for neutron data / °	6.0 to 155.95
restraints/parameters	56/113
Combined R_{wp} / R_{exp} / R_I	14.8%, 3.6%, 10.8%

Table S3b. Fractional atomic coordinates and equivalent isotropic displacement parameters (Å^2) for phase III of C_6H_6:C_6F_6. U_{eq} is defined as ⅓ of the trace of the orthogonalised U_{ij} tensor.

Atom	*x*	*y*	*z*	*U*(eq)
C(1)	−0.1948(9)	0.0563(4)	−0.0899(9)	7.1
C(2)	−0.0234(8)	0.1243(4)	−0.0133(8)	7.5
C(3)	0.1660(8)	0.0797(4)	0.0530(8)	7.2
C(4)	0.1819(9)	−0.0332(4)	0.0487(9)	7.1
C(5)	0.0101(8)	−0.1010(4)	−0.0262(8)	7.5
C(6)	−0.1786(9)	−0.0564(4)	−0.0952(16)	7.2
F(1)	−0.3827(10)	0.1013(5)	−0.1641(12)	10.3
F(2)	−0.0404(11)	0.2376(5)	−0.0064(13)	12.1
F(3)	0.3423(10)	0.1481(5)	0.1208(11)	10.8
F(4)	0.3699(10)	−0.0781(5)	0.1228(11)	10.3
F(5)	0.0253(12)	−0.2143(5)	−0.0287(14)	12.1
F(6)	−0.3523(12)	−0.1247(5)	−0.1694(12)	10.7
C(7)	−0.2055(13)	0.0281(8)	0.4175(12)	6.2

C(8)	−0.0284(17)	0.0969(6)	0.4807(16)	6.6
C(9)	0.1659(14)	0.0524(8)	0.5382(12)	6.3
C(10)	0.1828(13)	−0.0610(8)	0.5339(13)	6.2
C(11)	0.0061(17)	−0.1297(6)	0.4697(15)	6.6
C(12)	−0.1875(13)	−0.0852(8)	0.4099(10)	6.3
D(7)	-0.346(2)	0.0599(12)	0.380(4)	11.0
D(8)	-0.040(3)	0.1779(10)	0.483(5)	12.3
D(9)	0.293(2)	0.1015(12)	0.581(3)	11.4
D(10)	0.322(2)	−0.0928(13)	0.575(3)	11.1
D(11)	0.018(3)	−0.2106(10)	0.468(4)	12.3
D(12)	−0.312(2)	−0.1343(12)	0.360(3)	11.3

Table S3c. Anisotropic displacement parameters (Å^2) for phase II of C_6H_6:C_6F_6 calculated from the refined T and L matrices for each molecule. Anisotropic displacement factor exponent has the form: $-2\pi^2[h^2a^{*2}U_{11}+2hka^*b^*U_{12}+\ldots]$.

Atom	U_{11}	U_{22}	U_{33}	U_{23}	U_{13}	U_{12}
C(1)	0.062	0.155	0.054	-0.019	0.034	-0.002
C(2)	0.086	0.133	0.068	-0.014	0.034	-0.012
C(3)	0.061	0.150	0.063	-0.020	0.038	-0.027
C(4)	0.062	0.155	0.054	-0.019	0.034	-0.002
C(5)	0.086	0.133	0.068	-0.014	0.034	-0.013
C(6)	0.061	0.150	0.063	-0.020	0.038	-0.027
F(1)	0.091	0.224	0.075	-0.033	0.019	0.040
F(2)	0.188	0.134	0.132	-0.014	0.018	-0.001
F(3)	0.088	0.204	0.111	-0.037	0.036	-0.062
F(4)	0.091	0.224	0.075	-0.033	0.019	0.040
F(5)	0.189	0.134	0.132	-0.013	0.018	-0.002
F(6)	0.088	0.202	0.110	-0.038	0.035	-0.061
C(7)	0.077	0.146	0.017	0.035	0.003	0.022
C(8)	0.100	0.116	0.042	0.046	0.017	0.008
C(9)	0.072	0.139	0.032	0.024	0.018	-0.007
C(10)	0.077	0.146	0.017	0.036	0.003	0.022
C(11)	0.100	0.116	0.042	0.046	0.017	0.008
C(12)	0.072	0.139	0.032	0.024	0.018	-0.006
D(7)	0.101	0.205	0.107	0.016	-0.027	0.056
D(8)	0.172	0.117	0.180	0.051	0.013	0.016
D(9)	0.090	0.183	0.152	-0.012	0.017	-0.030
D(10)	0.103	0.205	0.105	0.018	-0.029	0.057
D(11)	0.173	0.117	0.180	0.052	0.013	0.016
D(12)	0.090	0.183	0.149	-0.015	0.013	-0.028

Table S4a. Lattice parameter data obtained from a constrained Rietveld fit to the data shown in Fig. 1 (and Fig. S1) for phase IV of C_6D_6:C_6F_6 on the first heating cycle starting at 10 am.

T / K	a / Å	b / Å	c / Å	α / °	β / °	γ / °	V / Z / Å^3
9.9	9.468(2)	7.407(2)	7.505(1)	90	95.62(1)	90	261.9(1)
10.7	9.468(2)	7.407(1)	7.505(1)	90	95.63(1)	90	261.9(1)
11.5	9.468(2)	7.407(1)	7.505(1)	90	95.62(1)	90	261.9(1)
12.3	9.468(2)	7.407(2)	7.505(1)	90	95.62(1)	90	261.9(1)
13.1	9.469(2)	7.407(1)	7.505(1)	90	95.62(1)	90	261.9(1)
13.9	9.468(2)	7.407(1)	7.505(1)	90	95.63(1)	90	261.9(1)
14.7	9.470(2)	7.407(1)	7.505(1)	90	95.63(1)	90	262.0(1)
15.4	9.468(2)	7.408(1)	7.505(1)	90	95.63(1)	90	261.9(1)
16.2	9.469(2)	7.407(1)	7.505(1)	90	95.63(1)	90	261.9(1)
17.0	9.469(2)	7.408(1)	7.506(1)	90	95.63(1)	90	262.0(1)
17.8	9.470(2)	7.408(2)	7.506(1)	90	95.63(1)	90	262.0(1)
18.6	9.469(2)	7.408(2)	7.505(1)	90	95.63(1)	90	262.0(1)
19.4	9.470(2)	7.408(1)	7.506(1)	90	95.63(1)	90	262.0(1)
20.1	9.471(2)	7.409(1)	7.506(1)	90	95.63(1)	90	262.0(1)
20.9	9.470(2)	7.408(1)	7.506(1)	90	95.63(1)	90	262.0(1)
21.8	9.471(2)	7.408(1)	7.506(1)	90	95.63(1)	90	262.1(1)
22.6	9.471(2)	7.408(1)	7.506(1)	90	95.63(1)	90	262.1(1)
23.5	9.472(2)	7.409(1)	7.506(1)	90	95.64(1)	90	262.1(1)
24.3	9.472(2)	7.409(1)	7.506(1)	90	95.64(1)	90	262.1(1)
25.1	9.473(2)	7.409(1)	7.507(1)	90	95.64(1)	90	262.2(1)
26.0	9.472(2)	7.410(2)	7.507(1)	90	95.64(1)	90	262.1(1)
26.8	9.473(2)	7.410(1)	7.507(1)	90	95.65(1)	90	262.2(1)
27.7	9.473(2)	7.410(1)	7.506(1)	90	95.65(1)	90	262.2(1)
28.5	9.474(2)	7.411(1)	7.507(1)	90	95.65(1)	90	262.3(1)
29.4	9.473(2)	7.411(2)	7.507(1)	90	95.65(1)	90	262.2(1)
30.2	9.475(2)	7.411(2)	7.507(1)	90	95.65(1)	90	262.3(1)
31.1	9.475(2)	7.411(1)	7.507(1)	90	95.65(1)	90	262.3(1)
32.1	9.476(2)	7.412(2)	7.508(1)	90	95.66(1)	90	262.4(1)
33.2	9.477(2)	7.412(2)	7.508(1)	90	95.66(1)	90	262.4(1)
34.1	9.477(2)	7.412(2)	7.508(1)	90	95.66(1)	90	262.4(1)
35.1	9.477(2)	7.412(2)	7.508(1)	90	95.66(1)	90	262.4(1)
36.0	9.477(2)	7.412(2)	7.508(1)	90	95.66(1)	90	262.4(1)
37.0	9.478(2)	7.412(2)	7.509(1)	90	95.67(1)	90	262.5(1)
37.9	9.478(2)	7.413(2)	7.509(1)	90	95.67(1)	90	262.5(1)
38.9	9.479(2)	7.413(2)	7.509(1)	90	95.67(1)	90	262.5(1)
39.8	9.480(2)	7.413(2)	7.509(1)	90	95.67(1)	90	262.6(1)
40.9	9.480(2)	7.413(2)	7.510(1)	90	95.68(1)	90	262.6(1)
41.9	9.480(2)	7.414(2)	7.510(1)	90	95.68(1)	90	262.6(1)
42.9	9.482(2)	7.415(2)	7.510(1)	90	95.68(1)	90	262.7(1)
44.0	9.482(2)	7.415(2)	7.511(1)	90	95.69(1)	90	262.7(1)
45.0	9.483(2)	7.415(2)	7.511(1)	90	95.69(1)	90	262.8(1)
46.1	9.483(2)	7.415(2)	7.511(1)	90	95.69(1)	90	262.8(1)
47.2	9.484(2)	7.416(2)	7.512(1)	90	95.69(1)	90	262.9(1)
48.4	9.484(2)	7.416(2)	7.512(1)	90	95.69(1)	90	262.9(1)
49.6	9.486(2)	7.417(2)	7.513(1)	90	95.70(1)	90	263.0(1)
50.7	9.487(2)	7.417(2)	7.513(1)	90	95.70(1)	90	263.0(1)
51.6	9.486(2)	7.418(2)	7.514(1)	90	95.70(1)	90	263.1(1)
52.5	9.488(2)	7.418(2)	7.514(1)	90	95.71(1)	90	263.1(1)
53.3	9.488(2)	7.419(2)	7.515(1)	90	95.71(1)	90	263.2(1)
54.2	9.489(2)	7.419(2)	7.515(1)	90	95.72(1)	90	263.2(1)
55.0	9.491(2)	7.419(2)	7.516(1)	90	95.72(1)	90	263.3(1)
55.7	9.491(2)	7.419(2)	7.516(1)	90	95.72(1)	90	263.3(1)
56.5	9.491(2)	7.420(2)	7.516(1)	90	95.72(1)	90	263.4(1)
57.2	9.492(2)	7.420(2)	7.517(1)	90	95.72(1)	90	263.4(1)
58.0	9.493(2)	7.421(1)	7.517(1)	90	95.73(1)	90	263.5(1)
58.7	9.493(2)	7.422(2)	7.518(1)	90	95.74(1)	90	263.5(1)
59.5	9.494(2)	7.422(2)	7.518(1)	90	95.74(1)	90	263.5(1)
60.4	9.494(2)	7.422(2)	7.518(1)	90	95.74(1)	90	263.6(1)
61.2	9.495(2)	7.423(2)	7.519(1)	90	95.74(1)	90	263.6(1)

62.0	9.497(2)	7.423(2)	7.520(1)	90	95.74(1)	90	263.7(1)
62.8	9.497(2)	7.423(2)	7.520(1)	90	95.75(1)	90	263.7(1)
63.6	9.497(2)	7.423(2)	7.520(1)	90	95.75(1)	90	263.8(1)
64.5	9.497(2)	7.424(2)	7.521(1)	90	95.76(1)	90	263.8(1)
65.3	9.498(2)	7.424(2)	7.521(1)	90	95.76(1)	90	263.8(1)
66.1	9.499(2)	7.424(2)	7.521(1)	90	95.76(1)	90	263.9(1)
66.9	9.500(2)	7.424(1)	7.522(1)	90	95.76(1)	90	263.9(1)
67.7	9.501(2)	7.425(2)	7.522(1)	90	95.77(1)	90	264.0(1)
68.6	9.502(2)	7.425(2)	7.522(1)	90	95.77(1)	90	264.0(1)
69.4	9.502(2)	7.425(2)	7.523(1)	90	95.78(1)	90	264.0(1)
70.3	9.504(2)	7.426(2)	7.523(1)	90	95.78(1)	90	264.1(1)
71.1	9.503(2)	7.427(1)	7.524(1)	90	95.78(1)	90	264.2(1)
72.0	9.504(2)	7.427(1)	7.525(1)	90	95.78(1)	90	264.2(1)
72.8	9.505(2)	7.427(1)	7.525(1)	90	95.79(1)	90	264.2(1)
73.6	9.507(2)	7.428(2)	7.526(1)	90	95.79(1)	90	264.4(1)
74.5	9.507(2)	7.428(2)	7.526(1)	90	95.79(1)	90	264.3(1)
75.3	9.508(2)	7.429(2)	7.526(1)	90	95.81(1)	90	264.4(1)
76.1	9.509(2)	7.429(1)	7.527(1)	90	95.80(1)	90	264.5(1)
76.9	9.511(2)	7.429(2)	7.528(1)	90	95.81(1)	90	264.6(1)
77.8	9.510(2)	7.430(2)	7.529(1)	90	95.81(1)	90	264.6(1)
78.7	9.512(2)	7.430(2)	7.529(1)	90	95.82(1)	90	264.7(1)
79.5	9.512(2)	7.430(2)	7.529(1)	90	95.82(1)	90	264.7(1)
80.4	9.514(2)	7.431(2)	7.530(1)	90	95.83(1)	90	264.8(1)
81.3	9.514(2)	7.431(2)	7.530(1)	90	95.83(1)	90	264.8(1)
82.1	9.515(2)	7.432(2)	7.531(1)	90	95.84(1)	90	264.9(1)
83.0	9.515(2)	7.433(2)	7.531(1)	90	95.84(1)	90	264.9(1)
83.8	9.517(2)	7.433(2)	7.532(1)	90	95.84(1)	90	265.0(1)
84.7	9.517(2)	7.433(2)	7.533(1)	90	95.85(1)	90	265.0(1)
85.6	9.518(2)	7.434(2)	7.533(1)	90	95.85(1)	90	265.1(1)
86.4	9.519(2)	7.435(2)	7.534(1)	90	95.86(1)	90	265.2(1)
87.3	9.520(2)	7.435(2)	7.534(1)	90	95.86(1)	90	265.3(1)
88.2	9.522(2)	7.435(2)	7.535(1)	90	95.86(1)	90	265.3(1)
89.0	9.522(2)	7.436(2)	7.535(1)	90	95.87(1)	90	265.3(1)
89.9	9.523(2)	7.436(2)	7.536(1)	90	95.87(1)	90	265.4(1)
90.7	9.524(2)	7.437(2)	7.537(1)	90	95.88(1)	90	265.5(1)
91.6	9.525(2)	7.437(2)	7.537(1)	90	95.88(1)	90	265.5(1)
92.5	9.525(2)	7.437(2)	7.538(1)	90	95.88(1)	90	265.6(1)
93.3	9.527(2)	7.438(2)	7.539(1)	90	95.89(1)	90	265.7(1)
94.2	9.528(2)	7.439(2)	7.539(1)	90	95.90(1)	90	265.8(1)
95.1	9.528(2)	7.439(2)	7.540(1)	90	95.90(1)	90	265.8(1)
96.0	9.530(2)	7.440(2)	7.541(1)	90	95.90(1)	90	265.9(1)
96.8	9.530(2)	7.440(2)	7.541(1)	90	95.91(1)	90	265.9(1)
97.7	9.532(2)	7.441(2)	7.542(1)	90	95.91(1)	90	266.0(1)
98.6	9.532(2)	7.441(2)	7.542(1)	90	95.92(1)	90	266.0(1)
99.4	9.533(2)	7.441(2)	7.543(1)	90	95.92(1)	90	266.1(1)
100.3	9.533(2)	7.442(2)	7.543(1)	90	95.93(1)	90	266.1(1)
101.2	9.536(2)	7.443(2)	7.544(1)	90	95.93(1)	90	266.3(1)
102.1	9.536(2)	7.443(2)	7.545(1)	90	95.94(1)	90	266.3(1)
103.0	9.537(2)	7.444(2)	7.545(1)	90	95.94(1)	90	266.4(1)
103.8	9.537(2)	7.444(2)	7.546(1)	90	95.95(1)	90	266.4(1)
104.7	9.539(2)	7.444(2)	7.547(1)	90	95.95(1)	90	266.5(1)
105.6	9.540(2)	7.444(2)	7.547(1)	90	95.95(1)	90	266.6(1)
106.5	9.541(2)	7.445(2)	7.548(1)	90	95.96(1)	90	266.6(1)
107.4	9.543(2)	7.446(2)	7.549(1)	90	95.96(1)	90	266.7(1)
108.3	9.543(2)	7.447(2)	7.550(1)	90	95.97(1)	90	266.8(1)
109.2	9.544(2)	7.446(2)	7.550(1)	90	95.97(1)	90	266.8(1)
110.1	9.545(2)	7.447(2)	7.551(1)	90	95.98(1)	90	266.9(1)
111.0	9.547(2)	7.448(2)	7.551(1)	90	95.99(1)	90	267.0(1)
111.9	9.548(2)	7.448(2)	7.552(1)	90	95.99(1)	90	267.0(1)
112.9	9.549(2)	7.450(2)	7.553(1)	90	95.99(1)	90	267.2(1)
113.7	9.549(2)	7.450(2)	7.554(1)	90	96.01(1)	90	267.2(1)
114.6	9.551(2)	7.450(2)	7.554(1)	90	96.01(1)	90	267.3(1)
115.5	9.553(2)	7.451(2)	7.555(1)	90	96.01(1)	90	267.4(1)
116.3	9.553(2)	7.451(2)	7.556(1)	90	96.02(1)	90	267.4(1)
117.2	9.555(2)	7.452(2)	7.557(1)	90	96.02(1)	90	267.5(1)

118.2	9.554(2)	7.452(2)	7.557(1)	90	96.03(1)	90	267.5(1)
119.1	9.557(2)	7.454(2)	7.558(1)	90	96.03(1)	90	267.7(1)
119.9	9.558(2)	7.454(2)	7.558(1)	90	96.04(1)	90	267.7(1)
120.8	9.559(2)	7.454(2)	7.559(1)	90	96.04(1)	90	267.8(1)
121.7	9.560(2)	7.455(2)	7.560(1)	90	96.05(1)	90	267.9(1)
122.6	9.561(2)	7.456(2)	7.561(1)	90	96.05(1)	90	268.0(1)
123.5	9.563(2)	7.456(2)	7.561(1)	90	96.07(1)	90	268.1(1)
124.4	9.563(2)	7.456(2)	7.562(1)	90	96.07(1)	90	268.1(1)
125.3	9.564(2)	7.457(2)	7.563(1)	90	96.07(1)	90	268.2(1)
126.2	9.566(2)	7.457(2)	7.563(1)	90	96.08(1)	90	268.2(1)
127.1	9.567(2)	7.458(2)	7.564(1)	90	96.08(1)	90	268.3(1)
128.0	9.568(2)	7.459(2)	7.565(1)	90	96.09(1)	90	268.4(1)
128.9	9.568(2)	7.459(2)	7.566(1)	90	96.09(1)	90	268.5(1)
129.8	9.570(2)	7.461(2)	7.567(1)	90	96.10(1)	90	268.6(1)
130.7	9.571(2)	7.462(2)	7.568(1)	90	96.11(1)	90	268.7(1)
131.6	9.573(2)	7.462(2)	7.568(1)	90	96.11(1)	90	268.7(1)
132.6	9.574(2)	7.462(2)	7.569(1)	90	96.11(1)	90	268.8(1)
133.5	9.575(2)	7.463(2)	7.570(1)	90	96.13(1)	90	268.9(1)
134.4	9.578(2)	7.463(2)	7.571(1)	90	96.13(1)	90	269.0(1)
135.3	9.579(2)	7.464(2)	7.571(1)	90	96.14(1)	90	269.1(1)
136.2	9.579(2)	7.464(2)	7.571(1)	90	96.14(1)	90	269.1(1)
137.1	9.581(2)	7.465(2)	7.572(1)	90	96.15(1)	90	269.2(1)
138.0	9.582(2)	7.466(2)	7.573(1)	90	96.15(1)	90	269.3(1)
138.9	9.583(2)	7.467(2)	7.574(1)	90	96.17(1)	90	269.4(1)
139.8	9.584(2)	7.467(2)	7.575(1)	90	96.17(1)	90	269.5(1)
140.7	9.586(2)	7.468(2)	7.575(1)	90	96.18(1)	90	269.5(1)
141.7	9.586(2)	7.468(2)	7.576(1)	90	96.18(1)	90	269.6(1)
142.6	9.587(2)	7.469(2)	7.577(1)	90	96.19(1)	90	269.7(1)
143.6	9.589(2)	7.470(2)	7.578(1)	90	96.20(1)	90	269.8(1)
144.6	9.591(2)	7.470(2)	7.579(1)	90	96.20(1)	90	269.9(1)
145.5	9.591(2)	7.471(2)	7.579(1)	90	96.21(1)	90	270.0(1)
146.5	9.592(2)	7.471(2)	7.580(1)	90	96.22(1)	90	270.0(1)
147.5	9.595(2)	7.472(2)	7.581(1)	90	96.22(1)	90	270.2(1)
148.4	9.596(2)	7.473(2)	7.582(1)	90	96.23(1)	90	270.2(1)
149.4	9.597(2)	7.473(2)	7.582(1)	90	96.24(1)	90	270.3(1)
150.4	9.600(2)	7.475(2)	7.583(1)	90	96.24(1)	90	270.5(1)
151.3	9.601(2)	7.475(2)	7.583(1)	90	96.25(1)	90	270.5(1)
152.2	9.602(2)	7.476(2)	7.585(1)	90	96.26(1)	90	270.6(1)
153.2	9.604(2)	7.476(2)	7.585(1)	90	96.27(1)	90	270.7(1)
154.1	9.604(2)	7.477(2)	7.586(1)	90	96.27(1)	90	270.8(1)
155.0	9.605(2)	7.477(2)	7.586(1)	90	96.28(1)	90	270.8(1)
156.0	9.607(2)	7.478(2)	7.587(1)	90	96.29(1)	90	270.9(1)
156.8	9.609(2)	7.479(2)	7.588(1)	90	96.30(1)	90	271.0(1)
157.9	9.611(2)	7.480(2)	7.590(1)	90	96.30(1)	90	271.2(1)
158.8	9.611(2)	7.480(2)	7.590(1)	90	96.31(1)	90	271.2(1)
159.6	9.613(2)	7.481(2)	7.591(1)	90	96.31(1)	90	271.3(1)
160.5	9.615(2)	7.482(2)	7.591(1)	90	96.32(1)	90	271.4(1)
161.6	9.616(2)	7.483(2)	7.592(1)	90	96.33(1)	90	271.5(1)
162.4	9.618(2)	7.484(2)	7.593(1)	90	96.33(1)	90	271.6(1)
163.2	9.619(2)	7.484(2)	7.594(1)	90	96.34(1)	90	271.7(1)
164.4	9.621(2)	7.485(2)	7.595(1)	90	96.35(1)	90	271.8(1)
165.3	9.622(2)	7.485(2)	7.595(1)	90	96.36(1)	90	271.8(1)
166.1	9.622(2)	7.487(2)	7.596(1)	90	96.37(1)	90	271.9(1)
167.1	9.624(2)	7.487(2)	7.597(1)	90	96.37(1)	90	272.0(1)
168.2	9.625(2)	7.488(2)	7.598(1)	90	96.38(1)	90	272.1(1)
169.0	9.628(2)	7.489(2)	7.599(1)	90	96.39(1)	90	272.3(1)
169.8	9.628(2)	7.490(2)	7.599(1)	90	96.40(1)	90	272.3(1)
170.9	9.630(2)	7.490(2)	7.600(1)	90	96.40(1)	90	272.4(1)
171.9	9.631(3)	7.491(2)	7.601(1)	90	96.41(1)	90	272.5(1)
172.6	9.632(3)	7.492(2)	7.601(1)	90	96.42(1)	90	272.5(2)
173.6	9.634(3)	7.493(2)	7.602(1)	90	96.43(1)	90	272.7(1)
174.7	9.636(2)	7.494(2)	7.603(1)	90	96.44(1)	90	272.8(1)
175.6	9.637(3)	7.494(2)	7.604(1)	90	96.45(1)	90	272.8(2)
176.3	9.638(3)	7.495(2)	7.604(1)	90	96.46(1)	90	272.9(1)
177.4	9.639(3)	7.495(2)	7.605(1)	90	96.46(1)	90	273.0(2)

178.4	9.642(3)	7.497(2)	7.606(1)	90	96.47(1)	90	273.1(2)
179.2	9.643(3)	7.497(2)	7.606(1)	90	96.48(1)	90	273.2(2)
180.0	9.644(3)	7.499(2)	7.607(1)	90	96.49(1)	90	273.3(2)
181.1	9.647(3)	7.500(2)	7.609(1)	90	96.49(1)	90	273.5(2)
182.0	9.648(3)	7.501(2)	7.609(1)	90	96.50(1)	90	273.5(2)
182.8	9.650(3)	7.501(2)	7.609(1)	90	96.51(1)	90	273.6(2)
183.8	9.652(3)	7.502(2)	7.610(1)	90	96.52(1)	90	273.7(2)
184.9	9.654(3)	7.504(2)	7.611(1)	90	96.53(1)	90	273.9(2)
185.7	9.655(3)	7.504(2)	7.611(1)	90	96.54(1)	90	273.9(2)
186.5	9.657(3)	7.506(2)	7.612(2)	90	96.55(1)	90	274.1(2)
187.6	9.657(3)	7.506(2)	7.613(1)	90	96.55(1)	90	274.1(2)
188.5	9.660(3)	7.508(2)	7.614(2)	90	96.57(1)	90	274.3(2)
189.2	9.663(3)	7.508(2)	7.615(2)	90	96.58(1)	90	274.4(2)
190.2	9.663(3)	7.509(2)	7.615(2)	90	96.58(1)	90	274.4(2)
191.4	9.664(3)	7.510(2)	7.615(2)	90	96.59(1)	90	274.5(2)
192.2	9.667(3)	7.512(2)	7.616(2)	90	96.61(1)	90	274.7(2)
193.0	9.668(3)	7.513(2)	7.617(1)	90	96.62(1)	90	274.8(2)
194.1	9.670(3)	7.514(2)	7.618(2)	90	96.62(1)	90	274.9(2)
195.0	9.672(3)	7.515(2)	7.618(2)	90	96.63(1)	90	275.0(2)
195.8	9.673(3)	7.516(2)	7.619(2)	90	96.64(1)	90	275.1(2)
196.6	9.674(3)	7.517(2)	7.620(2)	90	96.66(1)	90	275.2(2)
197.8	9.677(3)	7.519(2)	7.620(2)	90	96.66(1)	90	275.3(2)
198.7	9.679(3)	7.520(2)	7.621(2)	90	96.67(1)	90	275.4(2)
199.5	9.681(3)	7.521(2)	7.622(2)	90	96.69(1)	90	275.6(2)
200.4	9.683(3)	7.522(2)	7.622(2)	90	96.70(1)	90	275.7(2)
201.4	9.684(3)	7.523(2)	7.622(2)	90	96.71(1)	90	275.8(2)
202.4	9.685(3)	7.524(2)	7.624(2)	90	96.72(1)	90	275.9(2)
203.2	9.688(3)	7.526(2)	7.624(2)	90	96.73(1)	90	276.0(2)
204.1	9.690(3)	7.527(2)	7.625(2)	90	96.74(1)	90	276.2(2)
205.1	9.692(3)	7.529(2)	7.626(2)	90	96.76(1)	90	276.3(2)
206.0	9.695(3)	7.531(3)	7.626(2)	90	96.77(2)	90	276.4(2)
206.9	9.697(3)	7.532(3)	7.626(2)	90	96.78(2)	90	276.6(2)
207.9	9.698(3)	7.533(3)	7.627(2)	90	96.79(2)	90	276.7(2)
208.9	9.700(4)	7.534(3)	7.627(2)	90	96.80(2)	90	276.7(2)
209.7	9.703(4)	7.535(3)	7.627(2)	90	96.81(2)	90	276.9(3)
210.6	9.703(5)	7.534(4)	7.626(3)	90	96.81(3)	90	276.8(3)
211.6	9.707(7)	7.535(5)	7.626(4)	90	96.82(3)	90	276.9(4)

Table S4b. Lattice parameter data obtained from a constrained Rietveld fit to the data shown in Fig. 1 (and Fig. S1) for phase III of C_6D_6:C_6F_6 on heating.

T / K	a / Å	b / Å	c / Å	α / °	β / °	γ / °	V / Z / Å^3
225.4	6.353(2)	12.293(7)	7.270(2)	93.92(3)	96.75(2)	91.84(3)	281.0(3)
226.2	6.354(2)	12.296(6)	7.271(2)	93.95(2)	96.77(2)	91.82(3)	281.2(3)
227.2	6.358(2)	12.297(6)	7.272(2)	93.96(2)	96.80(2)	91.80(3)	281.3(3)
228.1	6.360(2)	12.301(6)	7.273(2)	93.97(2)	96.83(2)	91.78(3)	281.6(3)
229.0	6.364(2)	12.301(6)	7.274(2)	93.98(2)	96.85(2)	91.75(3)	281.8(3)
229.9	6.367(2)	12.306(6)	7.276(2)	94.01(2)	96.88(2)	91.74(3)	282.1(3)
230.9	6.369(2)	12.306(6)	7.276(2)	94.00(2)	96.93(2)	91.71(3)	282.1(3)
231.8	6.373(2)	12.308(6)	7.277(2)	94.02(2)	96.95(2)	91.68(3)	282.4(3)
232.7	6.377(2)	12.310(6)	7.279(2)	94.03(2)	96.99(2)	91.67(3)	282.6(3)
233.7	6.379(2)	12.311(7)	7.279(2)	94.05(3)	97.02(2)	91.64(3)	282.7(3)
234.6	6.384(3)	12.317(7)	7.281(2)	94.06(3)	97.05(2)	91.59(3)	283.2(3)
235.6	6.387(3)	12.314(7)	7.281(2)	94.07(3)	97.09(2)	91.57(3)	283.2(3)
236.5	6.389(3)	12.317(7)	7.281(2)	94.09(3)	97.14(2)	91.53(3)	283.4(3)
237.5	6.392(3)	12.320(8)	7.282(2)	94.11(3)	97.17(2)	91.51(4)	283.6(3)
238.4	6.396(3)	12.321(8)	7.283(2)	94.11(3)	97.22(2)	91.49(4)	283.8(3)
239.3	6.400(3)	12.323(8)	7.284(2)	94.12(3)	97.26(2)	91.45(3)	284.0(3)
240.3	6.404(3)	12.325(8)	7.285(3)	94.13(3)	97.30(2)	91.41(4)	284.3(4)
241.2	6.408(3)	12.326(8)	7.285(3)	94.15(3)	97.34(2)	91.38(4)	284.4(4)
242.1	6.411(3)	12.323(9)	7.285(3)	94.15(3)	97.39(2)	91.35(4)	284.4(4)
243.1	6.415(3)	12.327(9)	7.286(3)	94.16(3)	97.44(2)	91.31(4)	284.7(4)
244.1	6.419(4)	12.329(9)	7.287(3)	94.17(3)	97.49(2)	91.28(4)	285.0(4)
244.9	6.423(4)	12.328(9)	7.287(3)	94.18(3)	97.53(2)	91.23(4)	285.1(4)
246.0	6.428(4)	12.329(9)	7.288(3)	94.17(3)	97.58(2)	91.19(4)	285.3(4)
246.9	6.431(4)	12.325(10)	7.287(3)	94.19(3)	97.63(2)	91.16(4)	285.3(4)
247.8	6.435(4)	12.328(10)	7.288(3)	94.18(3)	97.68(2)	91.13(4)	285.6(4)
248.7	6.440(4)	12.324(10)	7.287(3)	94.17(3)	97.73(2)	91.09(4)	285.7(4)
249.7	6.446(4)	12.329(10)	7.289(3)	94.16(4)	97.79(2)	91.07(4)	286.1(4)
250.6	6.449(4)	12.327(10)	7.288(3)	94.13(4)	97.83(2)	91.03(4)	286.1(4)

Table S4c. Lattice parameter data obtained from a constrained Rietveld fit to the data shown in Fig. 1 (and Fig. S1) for phase II of C_6D_6:C_6F_6 on heating.

T / K	a / Å	b / Å	c / Å	α / °	β / °	γ / °	V / Z / Å^3
259.1	6.545(4)	12.291(9)	7.279(3)	90	98.89(3)	90	289.3(4)
260.0	6.550(4)	12.293(9)	7.280(3)	90	98.95(3)	90	289.5(4)
260.9	6.555(3)	12.288(9)	7.279(3)	90	99.01(3)	90	289.5(4)
261.9	6.559(3)	12.287(9)	7.279(3)	90	99.10(3)	90	289.6(4)
262.8	6.565(4)	12.283(9)	7.279(3)	90	99.16(3)	90	289.7(4)
263.7	6.569(3)	12.278(9)	7.278(3)	90	99.24(3)	90	289.7(4)
264.6	6.573(3)	12.274(9)	7.277(3)	90	99.32(3)	90	289.7(4)
265.5	6.578(3)	12.273(9)	7.276(3)	90	99.40(3)	90	289.7(4)
266.5	6.585(4)	12.272(9)	7.277(3)	90	99.48(3)	90	290.0(4)
267.4	6.590(4)	12.267(9)	7.276(3)	90	99.57(3)	90	290.0(4)
268.3	6.596(3)	12.265(9)	7.275(3)	90	99.66(3)	90	290.1(4)
269.2	6.603(4)	12.259(9)	7.274(3)	90	99.75(3)	90	290.1(4)
270.1	6.610(4)	12.260(9)	7.274(3)	90	99.85(3)	90	290.4(4)
271.0	6.620(4)	12.261(9)	7.275(3)	90	99.94(3)	90	290.8(4)
272.0	6.628(4)	12.258(9)	7.274(3)	90	100.05(3)	90	291.0(4)
272.8	6.636(4)	12.256(10)	7.273(3)	90	100.16(3)	90	291.1(5)
273.7	6.649(4)	12.257(10)	7.274(3)	90	100.27(3)	90	291.7(5)
274.6	6.658(4)	12.252(10)	7.273(3)	90	100.39(3)	90	291.8(5)
275.6	6.669(4)	12.247(10)	7.272(3)	90	100.53(3)	90	292.0(5)
276.4	6.680(4)	12.239(11)	7.270(3)	90	100.67(3)	90	292.0(5)

Table S4d. Lattice parameter data obtained from whole pattern LeBail fitting to the data shown in Fig. 1 (and Fig. S1) for phase I of C_6D_6:C_6F_6 on heating.

T / K	a / Å	b / Å	c / Å	α / °	β / °	γ / °	V / Z / Å^3
285.4	11.936(5)	11.936(5)	7.208(5)	90	90	120	296.5(7)
285.8	11.936(5)	11.936(5)	7.210(5)	90	90	120	296.5(6)
286.2	11.936(5)	11.936(5)	7.211(5)	90	90	120	296.6(6)
286.4	11.941(5)	11.941(5)	7.213(5)	90	90	120	296.9(6)
286.7	11.945(5)	11.945(5)	7.217(5)	90	90	120	297.3(7)
286.9	11.946(5)	11.946(5)	7.217(5)	90	90	120	297.3(7)
287.1	11.944(5)	11.944(5)	7.217(5)	90	90	120	297.2(7)
287.4	11.944(5)	11.944(5)	7.218(5)	90	90	120	297.3(7)
287.5	11.944(5)	11.944(5)	7.219(4)	90	90	120	297.3(6)
287.8	11.948(5)	11.948(5)	7.220(5)	90	90	120	297.5(6)
287.9	11.964(4)	11.964(4)	7.226(4)	90	90	120	298.6(5)
288.0	11.965(4)	11.965(4)	7.227(4)	90	90	120	298.6(6)
288.2	11.969(4)	11.969(4)	7.228(4)	90	90	120	298.9(6)
288.2	11.970(4)	11.970(4)	7.229(4)	90	90	120	299.0(6)
288.3	11.979(4)	11.979(4)	7.232(4)	90	90	120	299.5(6)
288.4	11.975(4)	11.975(4)	7.231(4)	90	90	120	299.3(5)
288.4	11.973(4)	11.973(4)	7.230(4)	90	90	120	299.2(6)
288.5	11.973(4)	11.973(4)	7.231(4)	90	90	120	299.2(6)
288.5	11.970(4)	11.970(4)	7.230(4)	90	90	120	299.0(5)
288.6	11.972(4)	11.972(4)	7.231(4)	90	90	120	299.2(6)

Table S4e. Lattice parameter data obtained from whole pattern LeBail fitting to the data shown in Fig. 1 (and Fig. S1) for phase I of C_6D_6:C_6F_6 on cooling.

T / K	a / Å	b / Å	c / Å	α / °	β / °	γ / °	V / Z / Å^3
288.7	11.967(3)	11.967(3)	7.227(3)	90	90	120	298.8(4)
288.6	11.966(3)	11.966(3)	7.227(3)	90	90	120	298.7(4)
288.4	11.961(2)	11.961(2)	7.225(2)	90	90	120	298.4(3)
288.3	11.966(3)	11.966(3)	7.226(3)	90	90	120	298.7(4)
288.0	11.965(3)	11.965(3)	7.226(3)	90	90	120	298.7(4)
287.8	11.964(3)	11.964(3)	7.225(3)	90	90	120	298.5(4)
287.6	11.960(3)	11.960(3)	7.224(3)	90	90	120	298.3(4)
287.3	11.954(2)	11.954(2)	7.222(2)	90	90	120	297.9(3)
287.0	11.954(3)	11.954(3)	7.222(2)	90	90	120	297.9(3)
286.7	11.958(3)	11.958(3)	7.223(2)	90	90	120	298.2(3)
286.4	11.956(2)	11.956(2)	7.222(2)	90	90	120	298.0(3)
286.1	11.955(3)	11.955(3)	7.221(3)	90	90	120	297.9(4)
285.8	11.953(2)	11.953(2)	7.220(2)	90	90	120	297.8(3)
285.4	11.953(3)	11.953(3)	7.220(3)	90	90	120	297.8(4)
285.1	11.953(2)	11.953(2)	7.219(2)	90	90	120	297.7(3)
284.7	11.956(3)	11.956(3)	7.220(3)	90	90	120	298.0(4)
284.4	11.950(3)	11.950(3)	7.218(3)	90	90	120	297.5(4)
284.1	11.948(2)	11.948(2)	7.217(2)	90	90	120	297.4(3)
283.7	11.949(2)	11.949(2)	7.217(2)	90	90	120	297.4(3)
283.3	11.952(2)	11.952(2)	7.217(2)	90	90	120	297.6(3)
283.0	11.952(3)	11.952(3)	7.217(3)	90	90	120	297.6(4)
282.6	11.950(3)	11.950(3)	7.216(3)	90	90	120	297.5(4)
282.3	11.952(2)	11.952(2)	7.216(2)	90	90	120	297.5(3)
281.9	11.949(3)	11.949(3)	7.214(2)	90	90	120	297.4(3)
281.5	11.944(2)	11.944(2)	7.212(2)	90	90	120	297.0(3)
281.1	11.944(2)	11.944(2)	7.212(2)	90	90	120	297.0(3)
280.7	11.944(2)	11.944(2)	7.211(2)	90	90	120	296.9(3)
280.4	11.941(2)	11.941(2)	7.210(2)	90	90	120	296.8(3)
280.0	11.946(2)	11.946(2)	7.211(2)	90	90	120	297.0(3)
279.6	11.942(3)	11.942(3)	7.209(3)	90	90	120	296.8(4)
279.2	11.944(3)	11.944(3)	7.209(3)	90	90	120	296.9(3)
278.9	11.944(2)	11.944(2)	7.209(2)	90	90	120	296.9(3)
278.5	11.941(2)	11.941(2)	7.208(2)	90	90	120	296.7(3)
278.1	11.943(2)	11.943(2)	7.208(2)	90	90	120	296.8(3)
277.7	11.944(2)	11.944(2)	7.207(2)	90	90	120	296.8(3)
277.3	11.943(3)	11.943(3)	7.207(2)	90	90	120	296.7(3)
277.0	11.942(2)	11.942(2)	7.206(2)	90	90	120	296.6(3)
276.6	11.941(3)	11.941(3)	7.205(2)	90	90	120	296.5(3)
276.2	11.940(3)	11.940(3)	7.204(3)	90	90	120	296.5(3)
275.8	11.938(2)	11.938(2)	7.203(2)	90	90	120	296.3(3)
275.4	11.934(2)	11.934(2)	7.202(2)	90	90	120	296.1(3)
275.0	11.933(3)	11.933(3)	7.200(2)	90	90	120	296.0(3)
274.6	11.935(2)	11.935(2)	7.201(2)	90	90	120	296.1(3)
274.2	11.930(2)	11.930(2)	7.199(2)	90	90	120	295.8(3)
273.9	11.933(2)	11.933(2)	7.199(2)	90	90	120	295.9(3)
273.5	11.928(2)	11.928(2)	7.197(2)	90	90	120	295.6(3)
273.1	11.930(2)	11.930(2)	7.197(2)	90	90	120	295.7(3)
272.7	11.934(2)	11.934(2)	7.198(2)	90	90	120	295.9(3)
272.3	11.928(2)	11.928(2)	7.196(2)	90	90	120	295.6(3)
271.9	11.924(2)	11.924(2)	7.194(2)	90	90	120	295.3(3)
271.6	11.932(3)	11.932(3)	7.197(3)	90	90	120	295.8(3)
271.1	11.923(2)	11.923(2)	7.193(2)	90	90	120	295.2(3)

Table S4f. Lattice parameter data obtained from a constrained Rietveld fit to the data shown in Fig. 1 (and Fig. S1) for phase II of C_6D_6:C_6F_6 on cooling.

T / K	a / Å	b / Å	c / Å	α / °	β / °	γ / °	V / Z / Å^3
266.3	6.676(5)	12.250(12)	7.266(4)	90	100.53(4)	90	292.1(6)
265.9	6.669(5)	12.250(12)	7.266(4)	90	100.45(4)	90	291.9(5)
265.5	6.662(5)	12.256(12)	7.267(4)	90	100.36(4)	90	291.8(5)
265.1	6.656(5)	12.254(12)	7.267(4)	90	100.29(4)	90	291.6(6)
264.7	6.651(5)	12.255(12)	7.267(4)	90	100.22(4)	90	291.5(6)
264.3	6.646(5)	12.254(12)	7.268(4)	90	100.16(4)	90	291.3(6)
263.8	6.640(5)	12.258(12)	7.268(4)	90	100.11(4)	90	291.2(6)
263.6	6.636(5)	12.262(12)	7.269(4)	90	100.05(4)	90	291.2(6)
263.1	6.630(5)	12.256(12)	7.267(4)	90	99.99(4)	90	290.8(5)
262.8	6.625(5)	12.259(12)	7.268(4)	90	99.95(4)	90	290.7(5)
262.4	6.621(5)	12.261(12)	7.268(4)	90	99.89(4)	90	290.7(6)
262.0	6.618(5)	12.261(12)	7.268(4)	90	99.85(4)	90	290.6(5)
261.6	6.614(5)	12.259(12)	7.268(4)	90	99.81(4)	90	290.3(5)
261.2	6.612(5)	12.265(12)	7.269(4)	90	99.76(4)	90	290.4(5)
260.8	6.608(4)	12.264(11)	7.269(4)	90	99.71(4)	90	290.3(5)
260.4	6.605(4)	12.263(11)	7.269(4)	90	99.68(4)	90	290.2(5)
260.0	6.602(4)	12.262(11)	7.269(4)	90	99.64(4)	90	290.1(5)
259.6	6.599(4)	12.264(11)	7.269(4)	90	99.60(4)	90	290.0(5)
259.3	6.597(4)	12.264(11)	7.269(4)	90	99.56(4)	90	290.0(5)
258.8	6.593(4)	12.266(11)	7.269(4)	90	99.52(4)	90	289.9(5)
258.4	6.590(4)	12.266(11)	7.269(4)	90	99.48(4)	90	289.7(5)
258.1	6.588(4)	12.269(11)	7.269(4)	90	99.45(4)	90	289.8(5)
257.7	6.585(4)	12.269(11)	7.269(4)	90	99.41(4)	90	289.7(5)
257.3	6.583(4)	12.269(11)	7.269(4)	90	99.38(3)	90	289.6(5)
256.9	6.580(4)	12.267(11)	7.268(4)	90	99.36(4)	90	289.4(5)
256.5	6.578(4)	12.267(11)	7.268(4)	90	99.32(4)	90	289.4(5)
256.1	6.575(4)	12.267(11)	7.268(4)	90	99.29(4)	90	289.3(5)
255.7	6.574(4)	12.271(11)	7.269(4)	90	99.25(4)	90	289.4(5)
255.3	6.571(4)	12.269(11)	7.268(4)	90	99.23(3)	90	289.2(5)
255.0	6.570(4)	12.272(11)	7.270(4)	90	99.19(4)	90	289.3(5)
254.6	6.568(4)	12.274(11)	7.270(4)	90	99.17(4)	90	289.3(5)
254.2	6.567(4)	12.276(11)	7.270(4)	90	99.14(4)	90	289.3(5)
253.8	6.564(4)	12.273(11)	7.269(4)	90	99.12(4)	90	289.1(5)
253.3	6.562(4)	12.277(11)	7.270(4)	90	99.09(4)	90	289.1(5)
253.0	6.561(4)	12.276(11)	7.270(4)	90	99.06(4)	90	289.1(5)
252.6	6.559(4)	12.278(11)	7.270(4)	90	99.03(4)	90	289.1(5)
252.2	6.557(4)	12.279(11)	7.271(4)	90	99.01(4)	90	289.1(5)
251.8	6.554(4)	12.279(11)	7.270(4)	90	98.99(3)	90	288.9(5)
251.4	6.553(4)	12.281(11)	7.271(4)	90	98.96(3)	90	289.0(5)
251.0	6.551(4)	12.285(11)	7.272(4)	90	98.93(4)	90	289.0(5)
250.6	6.549(4)	12.284(11)	7.272(4)	90	98.91(4)	90	289.0(5)
250.2	6.548(4)	12.285(11)	7.271(4)	90	98.88(4)	90	288.9(5)
249.7	6.544(4)	12.284(11)	7.271(4)	90	98.86(4)	90	288.7(5)
249.4	6.542(4)	12.286(11)	7.271(4)	90	98.83(4)	90	288.7(5)
248.9	6.540(4)	12.287(11)	7.271(4)	90	98.81(4)	90	288.7(5)
248.6	6.538(4)	12.286(11)	7.271(4)	90	98.78(4)	90	288.6(5)
248.2	6.536(4)	12.287(11)	7.271(4)	90	98.75(4)	90	288.6(5)
247.9	6.535(4)	12.289(11)	7.271(4)	90	98.74(4)	90	288.6(5)
247.5	6.533(4)	12.288(11)	7.271(4)	90	98.72(4)	90	288.4(5)
247.2	6.530(4)	12.287(11)	7.270(4)	90	98.70(4)	90	288.3(5)
246.8	6.529(4)	12.287(11)	7.270(4)	90	98.67(4)	90	288.3(5)
246.4	6.528(4)	12.288(11)	7.270(4)	90	98.65(4)	90	288.2(5)
246.1	6.527(4)	12.290(11)	7.271(4)	90	98.63(4)	90	288.3(5)
245.7	6.523(4)	12.287(11)	7.269(4)	90	98.61(4)	90	288.1(5)
245.3	6.523(4)	12.288(11)	7.270(4)	90	98.58(4)	90	288.1(5)
244.9	6.521(4)	12.288(11)	7.270(4)	90	98.57(4)	90	288.0(5)
244.6	6.518(4)	12.288(11)	7.269(4)	90	98.55(4)	90	287.9(5)
244.2	6.518(4)	12.291(11)	7.270(4)	90	98.55(4)	90	288.0(5)

Table S4g. Lattice parameter data obtained from a constrained Rietveld fit to the data shown in Fig. 1 (and Fig. S1) for phase III of C_6D_6:C_6F_6 on cooling.

T / K	a / Å	b / Å	c / Å	α / °	β / °	γ / °	V / Z / Å^3
240.5	6.448(4)	12.332(10)	7.279(3)	94.03(4)	97.84(2)	91.02(5)	285.9(5)
240.1	6.446(4)	12.331(9)	7.280(3)	94.05(3)	97.83(2)	91.02(4)	285.8(4)
239.7	6.445(4)	12.328(9)	7.279(3)	94.08(3)	97.80(2)	91.04(4)	285.7(4)
239.3	6.441(4)	12.325(9)	7.278(3)	94.10(3)	97.78(2)	91.06(4)	285.4(4)
239.0	6.440(4)	12.327(9)	7.278(3)	94.11(3)	97.75(2)	91.08(4)	285.4(4)
238.6	6.436(4)	12.327(9)	7.278(3)	94.11(3)	97.73(2)	91.08(4)	285.2(4)
238.2	6.435(3)	12.328(8)	7.278(3)	94.12(3)	97.71(2)	91.09(4)	285.2(4)
237.7	6.433(3)	12.330(8)	7.278(3)	94.13(3)	97.70(2)	91.11(4)	285.2(4)
237.4	6.432(3)	12.332(8)	7.279(3)	94.14(3)	97.67(2)	91.12(4)	285.2(4)
237.0	6.429(3)	12.331(8)	7.278(3)	94.14(3)	97.66(2)	91.14(4)	285.0(4)
236.6	6.428(3)	12.334(8)	7.278(3)	94.14(3)	97.64(2)	91.15(4)	285.1(4)
236.2	6.426(3)	12.333(8)	7.277(3)	94.16(2)	97.62(2)	91.17(4)	284.9(4)
235.8	6.425(3)	12.333(8)	7.276(3)	94.15(2)	97.61(2)	91.17(4)	284.9(4)
235.4	6.423(3)	12.332(7)	7.277(2)	94.16(2)	97.59(2)	91.19(3)	284.8(3)
235.0	6.421(3)	12.329(8)	7.275(3)	94.16(2)	97.57(2)	91.20(4)	284.6(4)
234.7	6.419(3)	12.331(7)	7.276(2)	94.16(2)	97.55(2)	91.22(3)	284.6(3)
234.3	6.418(3)	12.334(8)	7.276(2)	94.16(2)	97.53(2)	91.23(3)	284.6(3)
233.9	6.417(3)	12.334(8)	7.276(2)	94.15(3)	97.52(2)	91.23(3)	284.6(4)
233.5	6.416(3)	12.333(8)	7.276(2)	94.16(3)	97.50(2)	91.25(3)	284.5(4)
233.2	6.413(3)	12.330(7)	7.274(2)	94.16(2)	97.48(2)	91.26(3)	284.2(3)
232.8	6.412(3)	12.332(8)	7.275(2)	94.16(3)	97.46(2)	91.29(3)	284.3(4)
232.4	6.412(3)	12.331(8)	7.274(3)	94.16(3)	97.44(2)	91.29(4)	284.2(4)
232.0	6.410(3)	12.329(8)	7.274(3)	94.16(2)	97.42(2)	91.29(4)	284.1(4)
231.6	6.408(3)	12.328(8)	7.273(3)	94.16(3)	97.41(2)	91.32(3)	284.0(4)
231.2	6.407(3)	12.331(8)	7.274(3)	94.15(3)	97.39(2)	91.33(3)	284.1(4)
230.8	6.405(3)	12.326(8)	7.273(3)	94.15(2)	97.36(2)	91.35(3)	283.8(4)
230.5	6.403(3)	12.325(7)	7.273(2)	94.16(3)	97.35(2)	91.37(3)	283.7(3)
230.0	6.402(3)	12.324(7)	7.272(2)	94.15(3)	97.34(2)	91.38(3)	283.7(3)
229.7	6.401(3)	12.322(7)	7.271(2)	94.14(2)	97.31(2)	91.40(3)	283.5(3)
229.3	6.399(3)	12.323(7)	7.271(2)	94.14(3)	97.30(2)	91.41(3)	283.5(3)
229.0	6.396(3)	12.320(7)	7.270(2)	94.14(3)	97.29(2)	91.43(3)	283.2(3)
228.5	6.396(3)	12.319(7)	7.270(2)	94.13(3)	97.27(2)	91.43(3)	283.2(3)
228.2	6.395(3)	12.321(7)	7.270(2)	94.13(3)	97.25(2)	91.45(3)	283.2(3)
227.7	6.392(3)	12.316(7)	7.268(2)	94.12(2)	97.23(2)	91.46(3)	282.9(3)
227.4	6.392(3)	12.318(7)	7.269(2)	94.11(3)	97.21(2)	91.47(3)	283.0(3)
227.1	6.389(3)	12.314(7)	7.268(2)	94.10(3)	97.20(2)	91.48(3)	282.7(3)
226.6	6.388(3)	12.313(7)	7.268(2)	94.11(2)	97.18(2)	91.50(3)	282.7(3)
226.2	6.388(3)	12.315(7)	7.268(2)	94.10(2)	97.17(2)	91.50(3)	282.8(3)
225.9	6.385(2)	12.313(6)	7.267(2)	94.10(2)	97.14(2)	91.51(3)	282.6(3)
225.4	6.385(2)	12.312(6)	7.267(2)	94.09(2)	97.13(2)	91.52(3)	282.5(3)
225.1	6.383(2)	12.311(6)	7.267(2)	94.08(2)	97.12(2)	91.54(3)	282.4(3)
224.7	6.382(3)	12.310(7)	7.267(2)	94.08(2)	97.10(2)	91.55(3)	282.3(3)
224.3	6.379(2)	12.309(7)	7.266(2)	94.08(2)	97.08(2)	91.56(3)	282.2(3)
223.9	6.379(2)	12.310(6)	7.266(2)	94.08(2)	97.07(2)	91.57(3)	282.2(3)
223.5	6.377(2)	12.306(6)	7.266(2)	94.06(2)	97.05(2)	91.59(3)	282.0(3)
223.1	6.376(2)	12.307(6)	7.265(2)	94.05(2)	97.04(2)	91.60(3)	282.0(3)
222.7	6.374(2)	12.306(6)	7.264(2)	94.05(2)	97.02(2)	91.60(3)	281.9(3)
222.4	6.373(2)	12.302(6)	7.264(2)	94.05(2)	97.01(2)	91.61(3)	281.7(3)
221.9	6.371(2)	12.303(7)	7.264(2)	94.04(2)	96.99(2)	91.62(3)	281.7(3)
221.6	6.371(2)	12.300(6)	7.263(2)	94.03(2)	96.97(2)	91.63(3)	281.6(3)
221.2	6.368(2)	12.300(6)	7.263(2)	94.03(2)	96.96(2)	91.65(3)	281.5(3)
220.8	6.368(2)	12.300(6)	7.263(2)	94.03(2)	96.95(1)	91.67(3)	281.5(3)
220.3	6.367(2)	12.297(6)	7.262(2)	94.01(2)	96.93(1)	91.66(3)	281.3(3)
220.0	6.364(2)	12.296(6)	7.261(2)	94.01(2)	96.92(1)	91.69(3)	281.1(3)
219.6	6.364(2)	12.298(6)	7.262(2)	94.01(2)	96.90(1)	91.70(3)	281.2(3)
219.2	6.362(2)	12.295(6)	7.261(2)	94.00(2)	96.89(1)	91.70(3)	281.0(3)

218.8	6.361(2)	12.295(6)	7.261(2)	93.99(2)	96.87(1)	91.71(3)	281.0(3)
218.5	6.359(2)	12.292(6)	7.260(2)	93.99(2)	96.87(1)	91.72(3)	280.8(3)
218.0	6.358(2)	12.294(6)	7.260(2)	93.99(2)	96.85(1)	91.75(3)	280.8(3)
217.7	6.357(2)	12.291(6)	7.259(2)	93.97(2)	96.84(1)	91.76(3)	280.7(3)
217.3	6.356(2)	12.287(6)	7.258(2)	93.97(2)	96.82(2)	91.76(3)	280.5(3)
216.9	6.354(2)	12.290(6)	7.259(2)	93.97(2)	96.81(1)	91.77(3)	280.5(3)
216.5	6.353(2)	12.289(6)	7.258(2)	93.97(2)	96.80(1)	91.79(3)	280.4(3)
216.1	6.351(2)	12.288(6)	7.258(2)	93.97(2)	96.79(2)	91.80(3)	280.4(3)
215.7	6.351(2)	12.287(6)	7.258(2)	93.96(2)	96.77(2)	91.79(3)	280.3(3)
215.3	6.349(2)	12.284(6)	7.256(2)	93.96(2)	96.77(2)	91.81(3)	280.1(3)
215.0	6.348(2)	12.286(6)	7.256(2)	93.95(2)	96.75(2)	91.82(3)	280.1(3)
214.6	6.348(2)	12.289(6)	7.258(2)	93.95(2)	96.74(2)	91.83(3)	280.2(3)
214.2	6.346(2)	12.285(6)	7.256(2)	93.96(2)	96.73(2)	91.85(3)	280.0(3)
213.8	6.346(2)	12.284(6)	7.256(2)	93.95(2)	96.72(2)	91.84(3)	279.9(3)
213.4	6.345(2)	12.285(6)	7.256(2)	93.95(2)	96.70(2)	91.86(3)	280.0(3)
213.0	6.342(2)	12.281(6)	7.254(2)	93.95(2)	96.70(2)	91.87(3)	279.7(3)
212.6	6.341(2)	12.279(6)	7.254(2)	93.93(2)	96.69(2)	91.86(3)	279.6(3)
212.3	6.340(2)	12.281(6)	7.254(2)	93.94(2)	96.68(2)	91.88(3)	279.6(3)
211.8	6.340(2)	12.281(6)	7.254(2)	93.94(2)	96.67(2)	91.89(3)	279.6(3)
211.5	6.339(2)	12.278(6)	7.253(2)	93.93(2)	96.66(2)	91.89(3)	279.4(3)
211.1	6.337(2)	12.280(6)	7.254(2)	93.94(2)	96.64(1)	91.91(3)	279.4(3)
210.6	6.337(2)	12.278(6)	7.253(2)	93.93(2)	96.64(2)	91.90(3)	279.4(3)
210.3	6.335(2)	12.278(6)	7.253(2)	93.93(2)	96.63(2)	91.92(3)	279.3(3)
209.9	6.334(2)	12.275(6)	7.251(2)	93.93(2)	96.62(2)	91.92(3)	279.1(3)
209.5	6.333(2)	12.277(6)	7.252(2)	93.93(2)	96.61(2)	91.92(3)	279.1(3)
209.1	6.333(2)	12.278(6)	7.253(2)	93.93(2)	96.60(2)	91.92(3)	279.2(3)
208.7	6.332(2)	12.277(6)	7.252(2)	93.91(2)	96.59(1)	91.93(3)	279.2(3)
208.3	6.331(2)	12.275(6)	7.251(2)	93.92(2)	96.58(2)	91.94(3)	279.0(3)
207.9	6.329(2)	12.274(6)	7.251(2)	93.91(2)	96.58(2)	91.94(3)	278.9(3)
207.6	6.329(2)	12.276(6)	7.251(2)	93.91(2)	96.57(2)	91.95(3)	278.9(3)
207.2	6.328(2)	12.274(6)	7.250(2)	93.91(2)	96.56(2)	91.94(3)	278.8(3)
206.8	6.327(2)	12.274(6)	7.250(2)	93.91(2)	96.55(2)	91.95(3)	278.8(3)
206.4	6.326(2)	12.273(7)	7.250(2)	93.91(2)	96.53(2)	91.95(3)	278.7(3)
206.0	6.326(2)	12.272(6)	7.249(2)	93.90(2)	96.53(2)	91.96(3)	278.6(3)
205.6	6.324(2)	12.270(6)	7.249(2)	93.90(2)	96.52(2)	91.96(3)	278.5(3)
205.2	6.324(2)	12.270(6)	7.248(2)	93.89(2)	96.51(2)	91.96(3)	278.5(3)
204.8	6.322(2)	12.269(6)	7.248(2)	93.89(2)	96.50(2)	91.96(3)	278.4(3)
204.4	6.319(2)	12.267(7)	7.247(2)	93.89(2)	96.50(2)	91.98(3)	278.2(3)
204.0	6.319(2)	12.268(6)	7.247(2)	93.88(2)	96.49(2)	91.97(3)	278.2(3)
203.6	6.320(2)	12.269(6)	7.247(2)	93.89(2)	96.47(2)	91.98(3)	278.3(3)
203.3	6.319(2)	12.266(6)	7.246(2)	93.88(2)	96.47(2)	91.99(3)	278.1(3)
202.8	6.317(2)	12.266(6)	7.246(2)	93.87(2)	96.47(2)	91.98(3)	278.1(3)
202.4	6.317(2)	12.265(7)	7.246(2)	93.88(2)	96.45(2)	91.99(3)	278.0(3)
201.8	6.316(2)	12.265(6)	7.245(2)	93.88(2)	96.44(2)	92.00(3)	278.0(3)
201.3	6.314(2)	12.264(6)	7.245(2)	93.87(2)	96.44(2)	92.00(3)	277.9(3)
200.8	6.314(2)	12.265(6)	7.245(2)	93.88(2)	96.42(2)	92.01(3)	277.9(3)
200.5	6.313(2)	12.264(6)	7.244(2)	93.87(2)	96.42(2)	92.01(3)	277.8(3)
200.0	6.311(2)	12.265(7)	7.245(2)	93.88(2)	96.41(2)	92.02(3)	277.7(3)
199.5	6.310(2)	12.258(6)	7.242(2)	93.87(2)	96.40(2)	92.02(3)	277.5(3)
199.0	6.310(2)	12.261(6)	7.243(2)	93.86(2)	96.40(2)	92.01(3)	277.6(3)
198.7	6.308(2)	12.258(6)	7.242(2)	93.86(2)	96.39(2)	92.02(3)	277.4(3)
198.2	6.309(2)	12.261(6)	7.243(2)	93.86(2)	96.37(2)	92.01(3)	277.5(3)
197.8	6.306(2)	12.257(7)	7.241(2)	93.87(2)	96.36(2)	92.02(3)	277.2(3)
197.3	6.306(2)	12.258(6)	7.242(2)	93.87(2)	96.36(2)	92.04(3)	277.3(3)
196.9	6.305(2)	12.256(6)	7.241(2)	93.85(2)	96.36(2)	92.02(3)	277.1(3)
196.6	6.304(2)	12.256(6)	7.241(2)	93.86(2)	96.34(2)	92.03(3)	277.1(3)
196.2	6.303(2)	12.256(6)	7.240(2)	93.86(2)	96.34(2)	92.04(3)	277.1(3)
195.7	6.301(2)	12.256(7)	7.239(2)	93.86(2)	96.33(2)	92.05(3)	276.9(3)
195.3	6.302(2)	12.253(6)	7.239(2)	93.85(2)	96.32(2)	92.03(3)	276.9(3)
194.9	6.300(2)	12.250(6)	7.238(2)	93.85(2)	96.32(2)	92.05(3)	276.7(3)
194.5	6.300(2)	12.253(6)	7.239(2)	93.85(2)	96.30(2)	92.05(3)	276.8(3)

194.1	6.299(2)	12.253(6)	7.238(2)	93.85(2)	96.30(2)	92.04(3)	276.8(3)
193.7	6.298(3)	12.250(7)	7.237(2)	93.85(2)	96.29(2)	92.05(3)	276.6(3)
193.4	6.297(2)	12.250(6)	7.237(2)	93.86(2)	96.28(2)	92.07(3)	276.6(3)
193.0	6.296(2)	12.253(7)	7.237(2)	93.86(2)	96.27(2)	92.06(3)	276.6(3)
192.5	6.296(2)	12.251(7)	7.237(2)	93.86(2)	96.27(2)	92.06(3)	276.5(3)
192.2	6.295(2)	12.249(6)	7.236(2)	93.85(2)	96.26(2)	92.08(3)	276.4(3)
191.9	6.295(2)	12.248(7)	7.236(2)	93.85(2)	96.26(2)	92.07(3)	276.4(3)
191.6	6.294(3)	12.246(7)	7.235(2)	93.85(3)	96.25(2)	92.08(3)	276.3(3)
191.1	6.293(2)	12.247(7)	7.235(2)	93.84(2)	96.24(2)	92.06(3)	276.3(3)
190.7	6.293(2)	12.246(7)	7.234(2)	93.85(2)	96.23(2)	92.07(3)	276.2(3)
190.4	6.292(3)	12.246(7)	7.234(2)	93.85(3)	96.23(2)	92.08(3)	276.2(3)
190.1	6.291(3)	12.244(7)	7.234(2)	93.84(2)	96.22(2)	92.07(3)	276.1(3)
189.7	6.291(2)	12.245(7)	7.234(2)	93.85(2)	96.22(2)	92.08(3)	276.1(3)
189.3	6.289(2)	12.244(7)	7.233(2)	93.85(2)	96.22(2)	92.08(3)	276.0(3)
189.0	6.288(3)	12.242(7)	7.232(2)	93.85(3)	96.21(2)	92.08(3)	275.9(3)
188.6	6.288(3)	12.242(7)	7.232(2)	93.85(3)	96.20(2)	92.08(3)	275.8(3)
188.2	6.287(3)	12.239(7)	7.231(3)	93.85(2)	96.20(2)	92.10(4)	275.6(3)
187.7	6.287(3)	12.240(7)	7.231(2)	93.84(3)	96.19(2)	92.09(3)	275.7(3)
187.5	6.285(3)	12.239(7)	7.231(2)	93.85(3)	96.18(2)	92.09(3)	275.6(3)
187.2	6.285(3)	12.238(7)	7.230(2)	93.85(3)	96.18(2)	92.09(3)	275.5(3)
186.8	6.285(3)	12.238(7)	7.230(2)	93.85(3)	96.17(2)	92.10(3)	275.5(3)
186.3	6.283(3)	12.235(7)	7.229(3)	93.85(3)	96.16(2)	92.10(4)	275.4(3)
185.9	6.283(3)	12.236(7)	7.229(2)	93.85(3)	96.16(2)	92.11(3)	275.4(3)
185.6	6.282(3)	12.237(7)	7.229(2)	93.86(3)	96.15(2)	92.12(3)	275.3(3)
185.2	6.282(3)	12.236(7)	7.229(2)	93.85(3)	96.14(2)	92.11(3)	275.4(3)
184.7	6.280(3)	12.235(7)	7.228(3)	93.86(3)	96.14(2)	92.11(3)	275.2(3)
184.3	6.279(3)	12.231(8)	7.226(3)	93.85(3)	96.14(2)	92.11(4)	275.0(3)
184.0	6.279(3)	12.233(7)	7.227(3)	93.85(3)	96.13(2)	92.12(3)	275.1(3)
183.5	6.278(3)	12.232(7)	7.227(3)	93.85(3)	96.12(2)	92.12(3)	275.0(3)
183.1	6.278(3)	12.232(7)	7.226(2)	93.86(3)	96.12(2)	92.13(3)	274.9(3)
182.7	6.278(3)	12.233(7)	7.226(3)	93.86(3)	96.11(2)	92.12(3)	275.0(3)
182.4	6.276(3)	12.228(8)	7.225(3)	93.86(3)	96.10(2)	92.13(4)	274.8(4)
181.9	6.275(3)	12.231(7)	7.225(3)	93.86(3)	96.10(2)	92.13(3)	274.8(3)
181.5	6.276(3)	12.232(7)	7.226(3)	93.86(3)	96.09(2)	92.13(3)	274.9(3)
181.2	6.274(3)	12.229(7)	7.224(3)	93.86(3)	96.08(2)	92.13(3)	274.7(3)
180.8	6.273(3)	12.226(7)	7.223(3)	93.86(3)	96.08(2)	92.13(3)	274.5(3)
180.4	6.271(3)	12.224(8)	7.223(3)	93.86(3)	96.07(2)	92.14(4)	274.4(4)
179.9	6.272(3)	12.225(7)	7.223(3)	93.86(3)	96.06(2)	92.14(3)	274.5(3)
179.5	6.272(3)	12.226(8)	7.223(3)	93.85(3)	96.06(2)	92.13(3)	274.5(3)
179.2	6.272(3)	12.228(8)	7.223(3)	93.86(3)	96.06(2)	92.14(3)	274.5(3)
178.8	6.271(3)	12.227(8)	7.224(3)	93.86(3)	96.05(2)	92.14(3)	274.5(3)
178.4	6.270(3)	12.228(8)	7.224(3)	93.86(3)	96.04(2)	92.15(4)	274.5(4)
177.9	6.269(3)	12.224(8)	7.222(3)	93.86(3)	96.04(2)	92.15(3)	274.3(4)
177.6	6.268(3)	12.224(8)	7.221(3)	93.86(3)	96.03(2)	92.14(3)	274.2(3)
177.3	6.267(3)	12.222(8)	7.221(3)	93.87(3)	96.02(2)	92.16(3)	274.1(4)
176.8	6.266(3)	12.222(8)	7.220(3)	93.88(3)	96.02(2)	92.16(3)	274.0(4)
176.4	6.265(3)	12.220(8)	7.219(3)	93.87(3)	96.01(2)	92.16(4)	273.9(4)
175.9	6.265(3)	12.220(8)	7.219(3)	93.86(3)	96.01(2)	92.15(3)	273.9(3)
175.7	6.265(3)	12.220(8)	7.219(3)	93.87(3)	96.00(2)	92.16(3)	273.9(4)
175.2	6.264(3)	12.221(8)	7.220(3)	93.87(3)	95.99(2)	92.16(4)	274.0(4)
174.8	6.264(3)	12.218(8)	7.219(3)	93.88(3)	95.98(2)	92.17(4)	273.8(4)
174.3	6.262(3)	12.216(8)	7.218(3)	93.87(3)	95.98(2)	92.17(4)	273.7(4)
174.0	6.262(3)	12.218(8)	7.218(3)	93.88(3)	95.98(2)	92.18(4)	273.7(4)
173.5	6.261(3)	12.218(8)	7.217(3)	93.87(3)	95.97(2)	92.17(4)	273.6(4)
173.1	6.260(3)	12.217(8)	7.217(3)	93.88(3)	95.96(2)	92.18(4)	273.6(4)
172.8	6.260(3)	12.217(8)	7.217(3)	93.87(3)	95.95(2)	92.17(4)	273.6(4)
172.5	6.258(3)	12.212(9)	7.215(3)	93.87(3)	95.96(2)	92.19(4)	273.3(4)
172.1	6.258(3)	12.214(8)	7.216(3)	93.86(3)	95.95(2)	92.20(4)	273.4(4)
171.6	6.257(3)	12.214(8)	7.215(3)	93.87(3)	95.94(2)	92.21(4)	273.3(4)
171.4	6.256(3)	12.212(9)	7.214(3)	93.86(3)	95.94(2)	92.21(4)	273.2(4)
171.1	6.255(3)	12.213(9)	7.215(3)	93.87(3)	95.94(2)	92.21(4)	273.2(4)

170.7	6.256(3)	12.211(9)	7.215(3)	93.85(3)	95.93(2)	92.21(4)	273.2(4)
170.2	6.256(3)	12.210(9)	7.215(3)	93.84(3)	95.93(2)	92.21(4)	273.2(4)
169.9	6.254(3)	12.209(9)	7.214(3)	93.84(3)	95.92(2)	92.22(4)	273.0(4)
169.6	6.253(3)	12.208(9)	7.215(3)	93.84(3)	95.92(2)	92.22(4)	273.0(4)
169.2	6.254(3)	12.210(9)	7.215(3)	93.82(3)	95.92(2)	92.23(4)	273.1(4)
168.8	6.254(4)	12.210(10)	7.216(3)	93.80(3)	95.91(2)	92.25(4)	273.2(4)

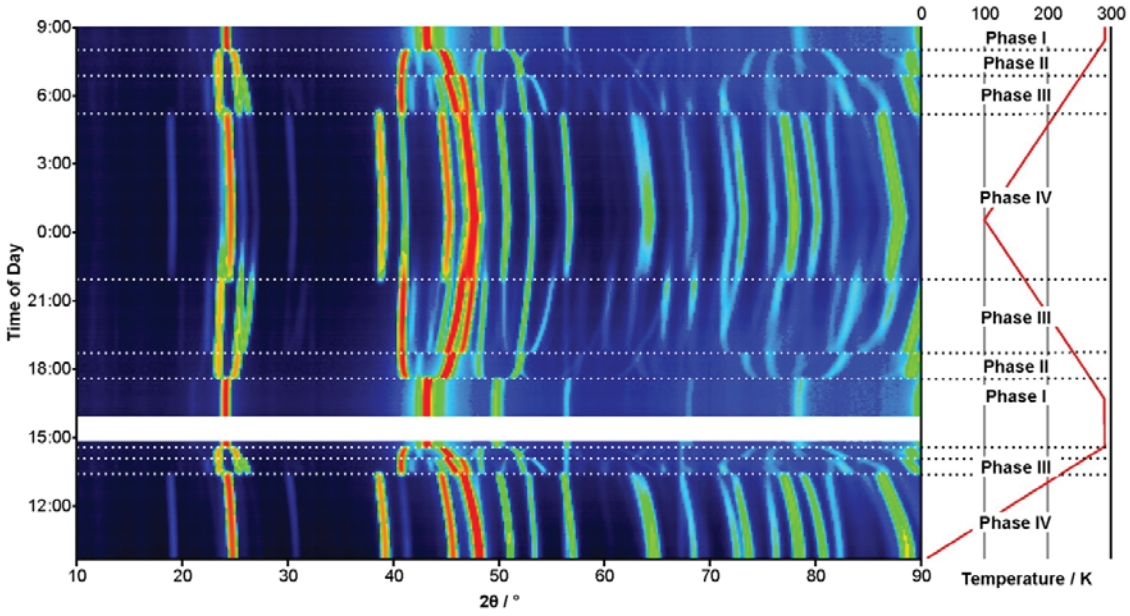

Fig. S1. PND data collected on a sample of C_6D_6:C_6F_6 as a function of both heating and cooling displayed as a surface plot to show diffraction intensity as a function of sample temperature (right-hand scale). Data were collected on D1B with λ = 2.52 Å (nominal). Neutron intensity is shown using a thermal-style colour scale going from blue (low intensity) via green and yellow to red (maximum intensity approx. 60,000 counts min^{-1}). The temperature regions for the 4 different phases are indicated on the right-hand scale. On cooling from phase III to phase IV, incomplete transformation is apparent, as easily seen for the intense peak from phase III at 2θ ≈ 41° which co-exists in the diffraction patterns of phase IV. Similar behaviour was observed in our recent experiments by laboratory PXRD. (Note: wire 381 on the detector at 86° in 2θ was found to be noisy; consequently, the plotted data were interpolated for this wire, and the fitted data were zero-weighted for this wire.)

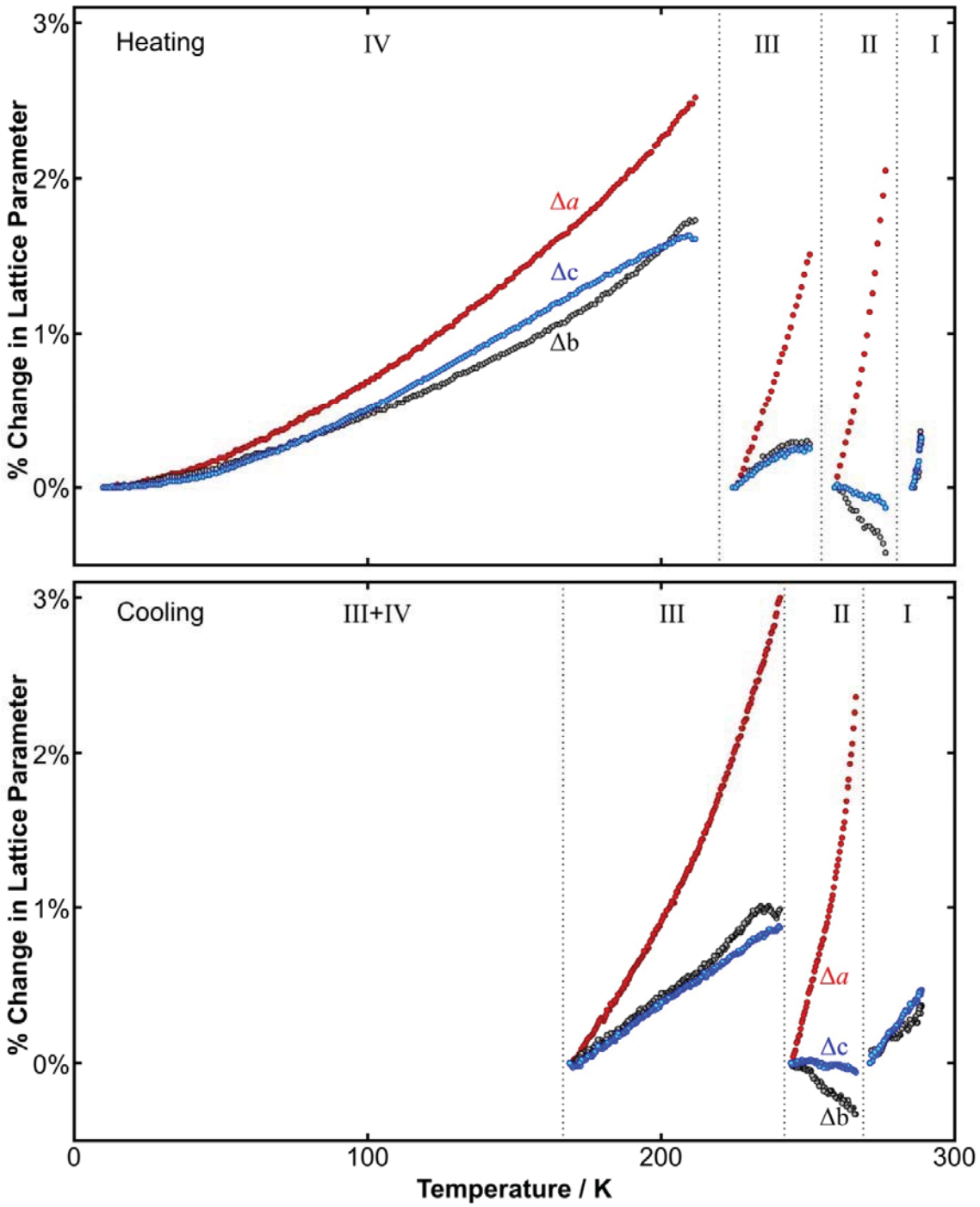

Fig. S2. Percentage change in lattice parameters *a*, *b*, and *c* in red, blue, and black points, respectively, as a function of temperature on heating (upper) and on cooling (lower) obtained from the data shown in Fig. 1. On cooling through the phase III-IV transition, residual phase III in the sample prevented accurate determination of the lattice parameters of phase IV from the data. The percentage change is calculated relative to the first diffraction pattern measured in the new phase on heating and to the last diffraction pattern on cooling.

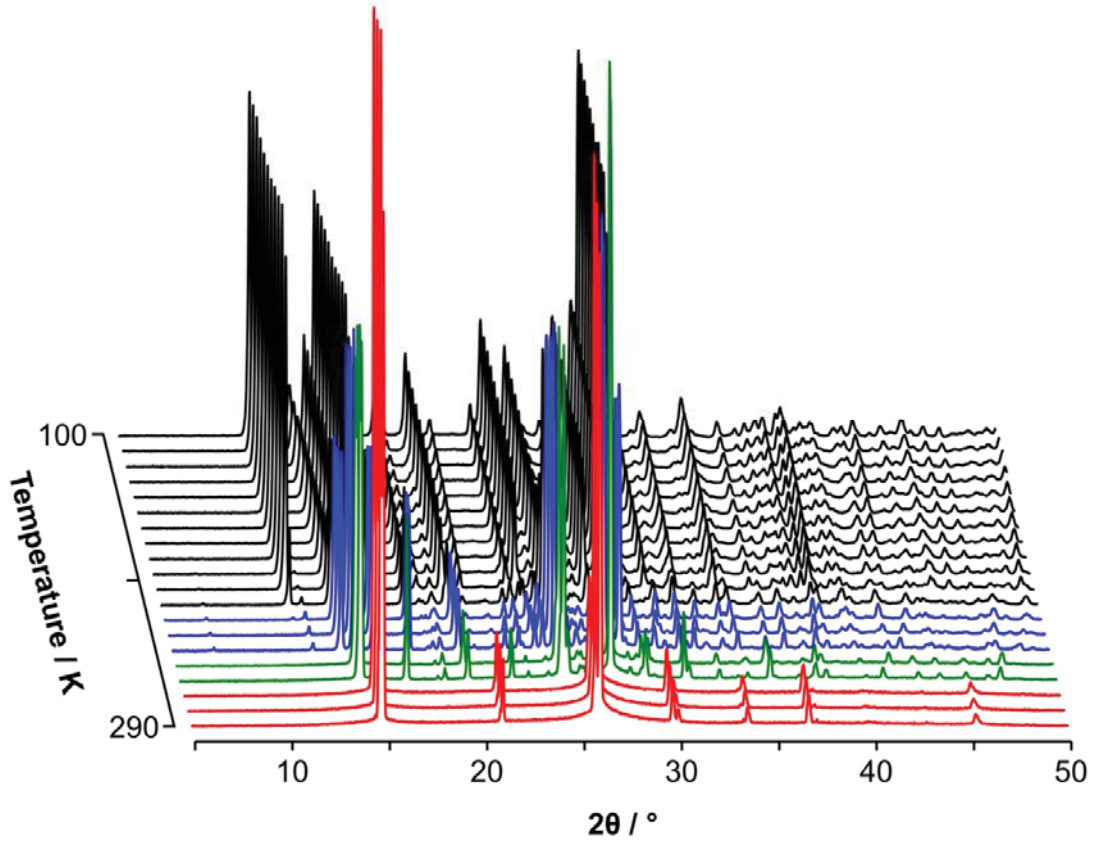

Fig. S3. Laboratory PXRD data of C_6F_6:C_6H_6 from 100 K to 290 K measured on a Stoe Stadi-P diffractometer with Cu Ka_1 radiation, λ = 1.54056 Å, showing the same 3 phase transitions as seen in the PND data collected some quarter of a century earlier. In marked contrast to the PND data, the sample at 100 K exhibits a significant amount of untransformed phase III. Strain broadening is evident in phase III from the increased width of the $\bar{1}10$ reflection at 100 K, which narrows as the sample is warmed up to 220 K.

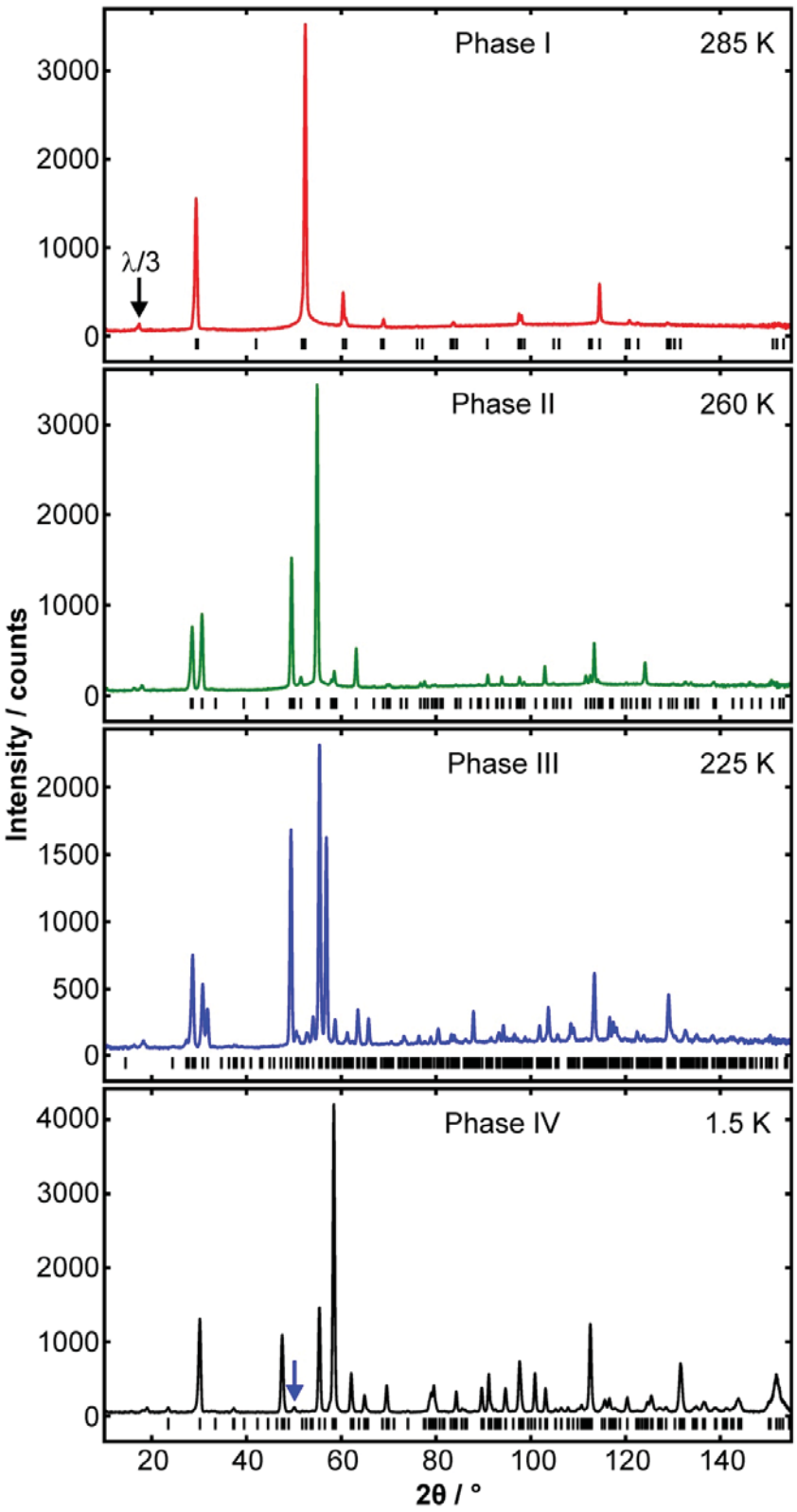

Fig. S4. PND data collected with λ = 2.997 Å on D1A at the ILL at 4 sample temperatures. Vertical tick marks indicate calculated reflections positions. A λ/3 contamination wavelength from the Ge(113) monochromator gives rise to harmonic peaks at low angle. Phase IV is nearly free of phase III as shown by a very weak phase III peak (indicated by blue arrow).

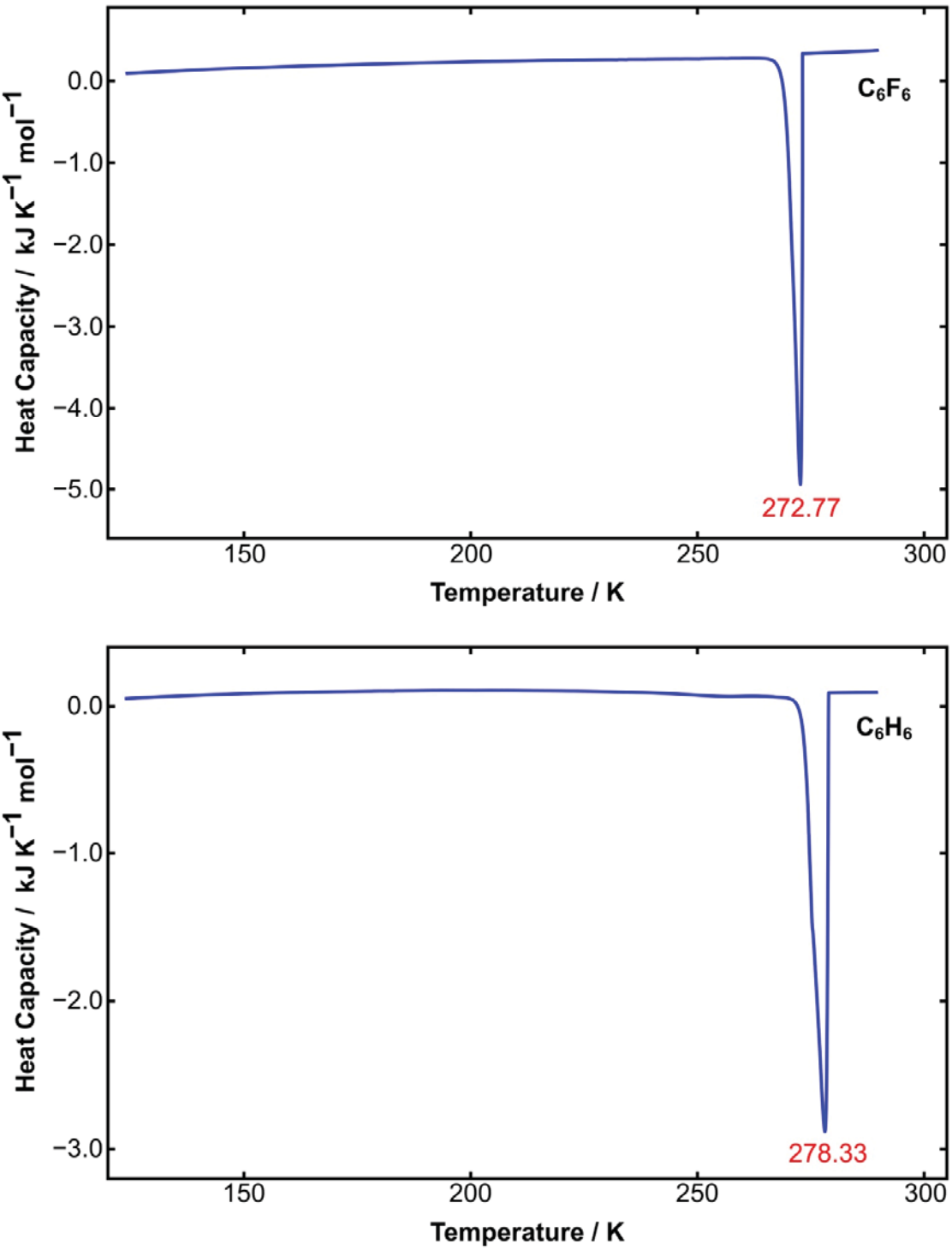

Fig. S5. DSC data for C_6F_6 (upper) and C_6H_6 (lower) on cooling measured using the same procedure as for the binary adduct. The temperatures of the two freezing-point transitions of the pure components closely matches the position of peaks seen in the DSC cooling trace of the binary adduct (Fig. 2).

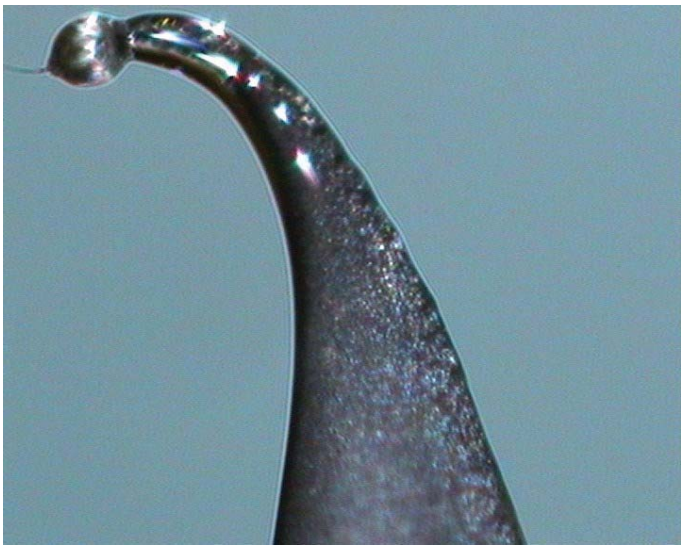

Fig. S6. C_6H_6:C_6F_6 was filled in a 0.5 mm capillary, flame sealed, and the sample was then condensed at the sealed end and allowed to anneal for 4 days on a twin-source Agilent SuperNova diffractometer equipped with a micro-focus Cu X-ray beam (50 kV, 0.8 mA) and an Atlas (135 mm CCD) detector. The sample temperature was held at 290 K, just below the melting point at 298 K, with an Oxford Instruments Cryojet5® to facilitate crystal growth. It was important to check that the capillary is 100% sealed to prevent loss of sample when kept at room temperature over many days.

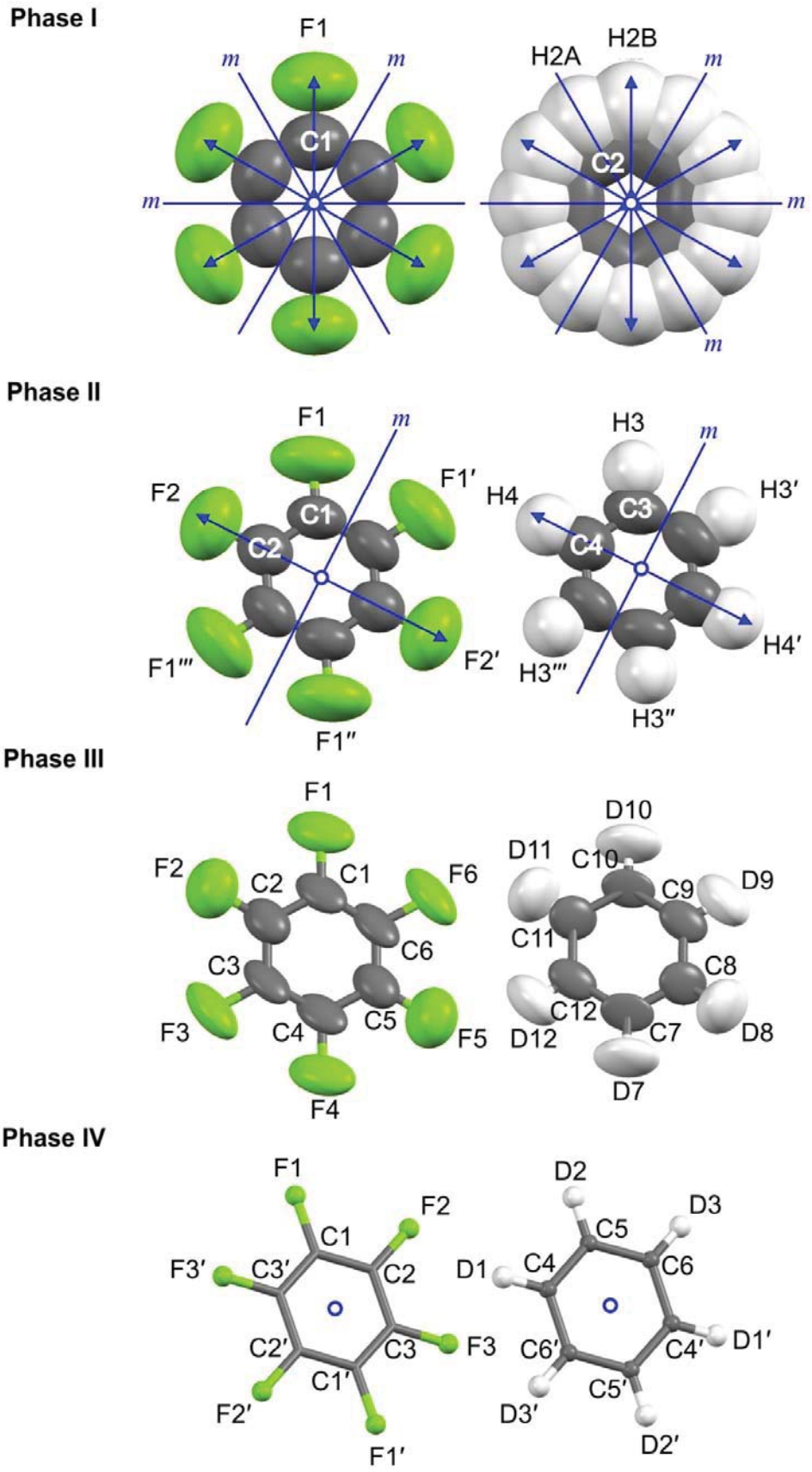

Fig. S7. Atomic labelling scheme used in the refinement of the four crystal structures of C_6H_6:C_6F_6. Molecular point-group symmetry elements are shown in blue.

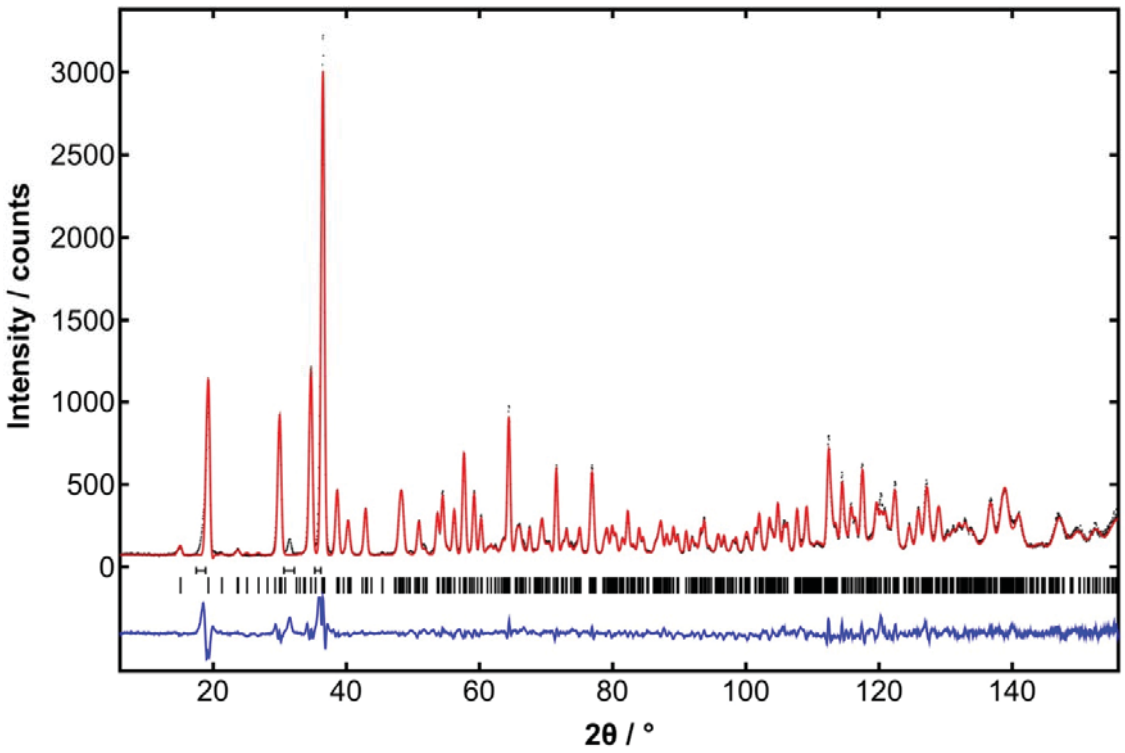

Fig. S8. Rietveld refinement fit to PND data of C_6F_6:C_6D_6 phase IV at 1.5 K measured on D1A at the ILL with λ = 1.9087 Å (as originally published in black and white[1]). Data is shown with black dots, calculated pattern as red curve, difference between observed and calculated as blue curve, and vertical tick marks show calculated reflections positions. Horizontal bars show small regions of the pattern excluded from the fit due to overlap with the most intense peaks from phase III.

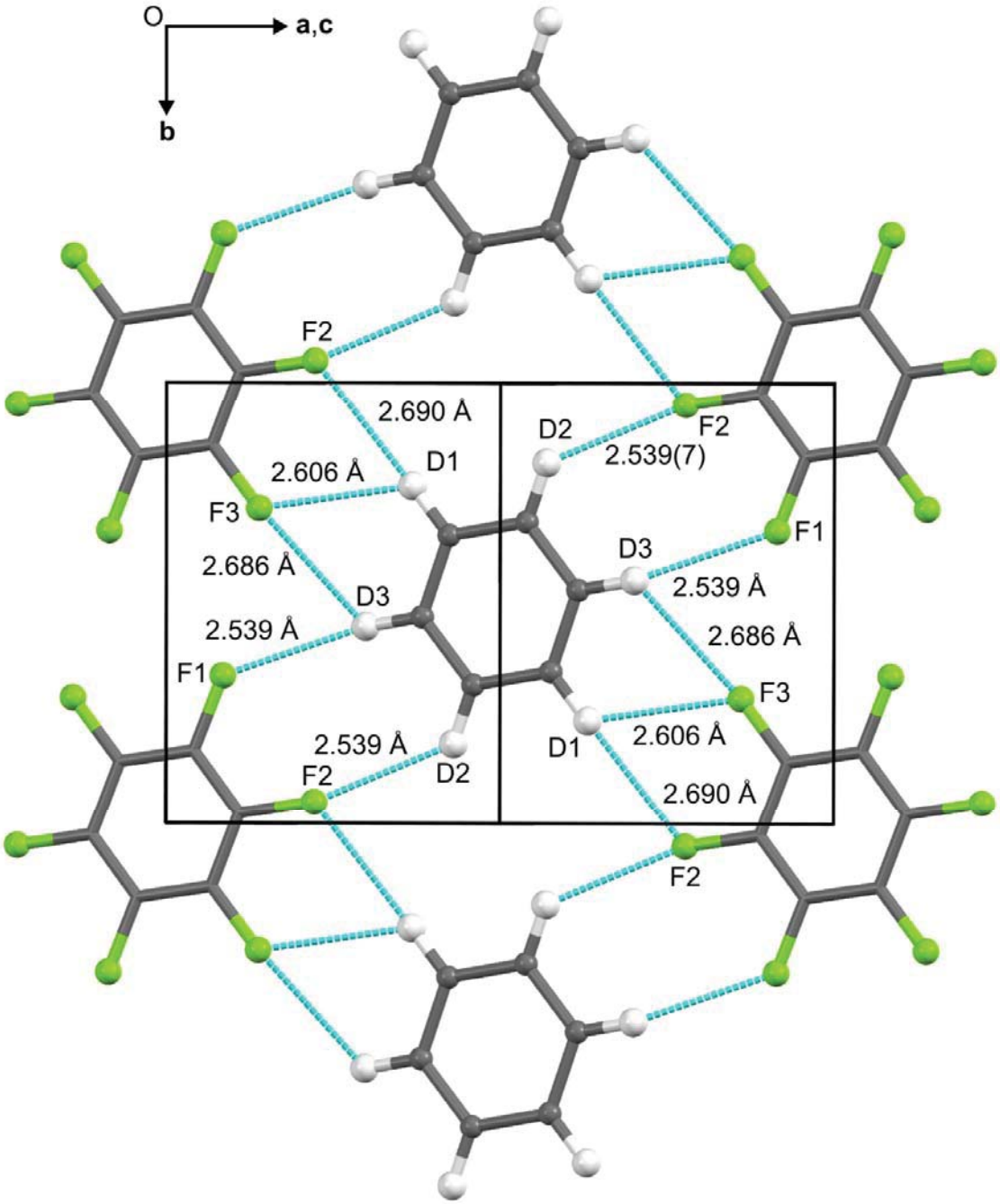

Fig. S9. Bond-dipole interactions within a plane crossing the unit cell in C_6H_6:C_6F_6 phase IV leading to sheets of molecules in addition to the columns formed in all four phases by the quadrupolar interactions between the π rings of the molecules. Standard uncertainty on the distances shown is 0.007 Å.

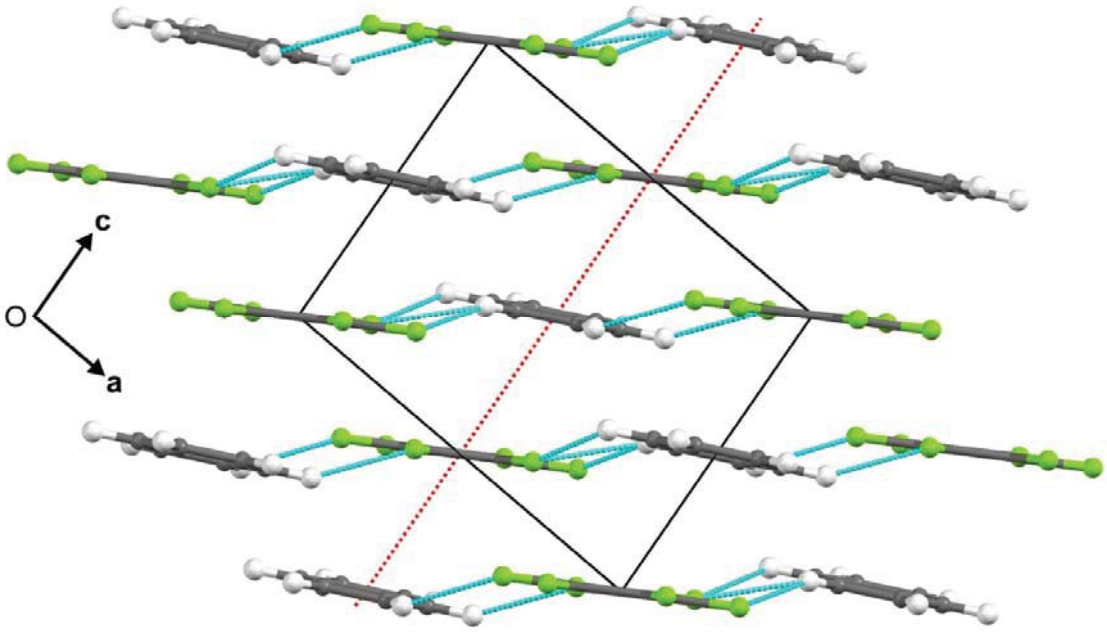

Fig. S10. Bond-dipole interactions viewed down the **b** axis in C_6H_6:C_6F_6 phase IV leading to sheets of molecules in addition to the columns (shown by the dotted red line) formed in all four phases by the quadrupolar interactions between the π rings of the molecules.

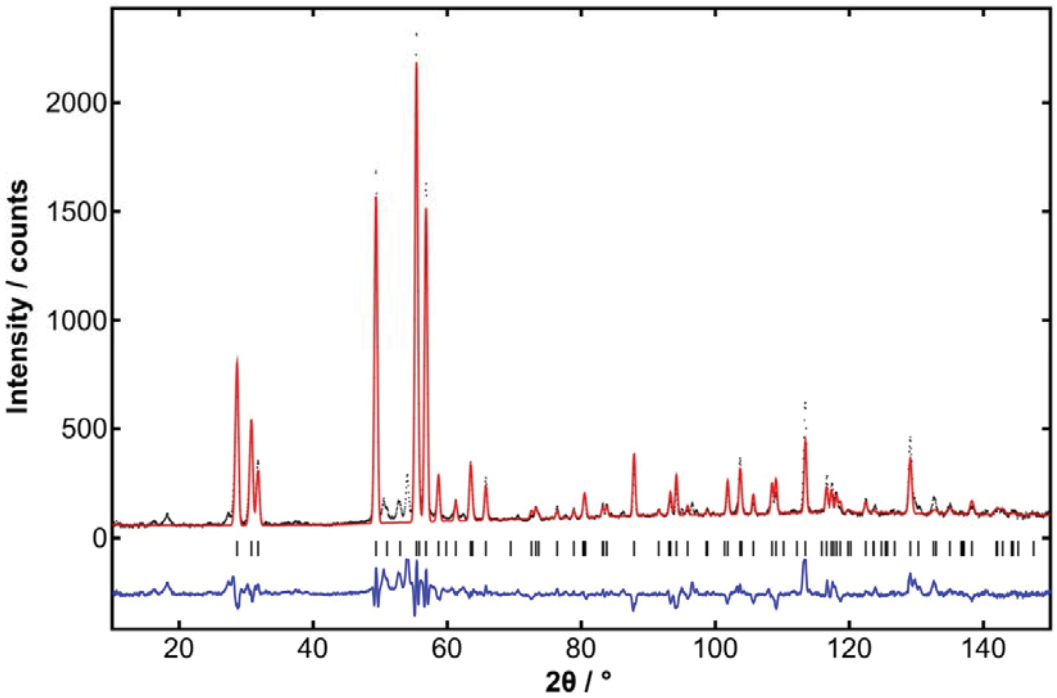

Fig. S11. Rietveld fit the neutron data of C_6F_6:C_6D_6 phase III at 225 K measured on D1A at the ILL with λ = 1.9087 Å. Data is shown with black dots, calculated pattern as red curve, difference between observed and calculated as blue curve, and vertical tick marks show calculated reflections positions. The fit is based on a C-centred sub-cell with a single "C_6F_6/C_6D_6" molecule. Most of the peak intensities can be accounted for with this approximate model.

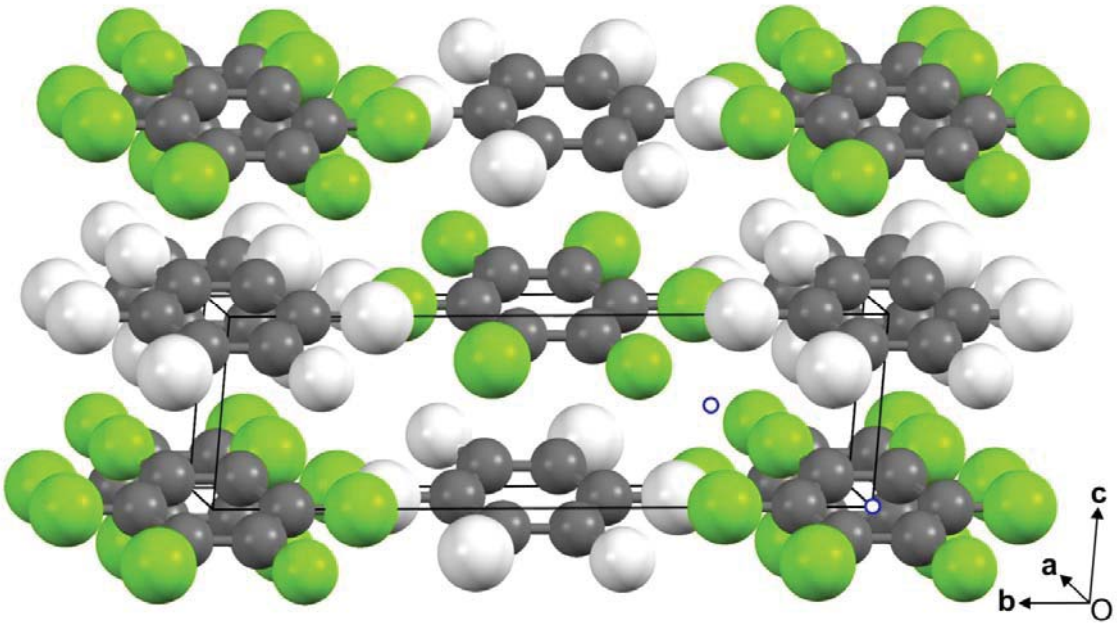

Fig. S12. View of the crystal structure of C_6H_6:C_6F_6 phase III as determined initially from Rietveld refinement using the PND data measured on D1A at 225 K and the C-centred sub-cell shown using a single "C_6F_6/C_6D_6" molecule. The true cell would be doubled along *c* giving rise to a structure with C_6F_6 and C_6H_6 molecules stacked eclipsed and alternately. In addition, the structure is approximately I-centred (as shown) given that the most of the scattering in the PXRD data arises from *hkl* reflections with *h*+*k*+*l* even. In space group $I\bar{1}$, there are two sets of inversion points: one set at (0,0,0) plus symmetry equivalent and the second set at (¼,¼,¼) plus symmetry equivalent (as shown by the open blue circles). In the correct space group of $P\bar{1}$ for C_6H_6:C_6F_6 phase III, only one set of inversion centres can be present in the structure: only the inversion centres relating symmetry equivalent molecules at (¼,¼,¼) plus symmetry equivalent ones remain, thus necessitating the use of a non-standard setting for phase III.

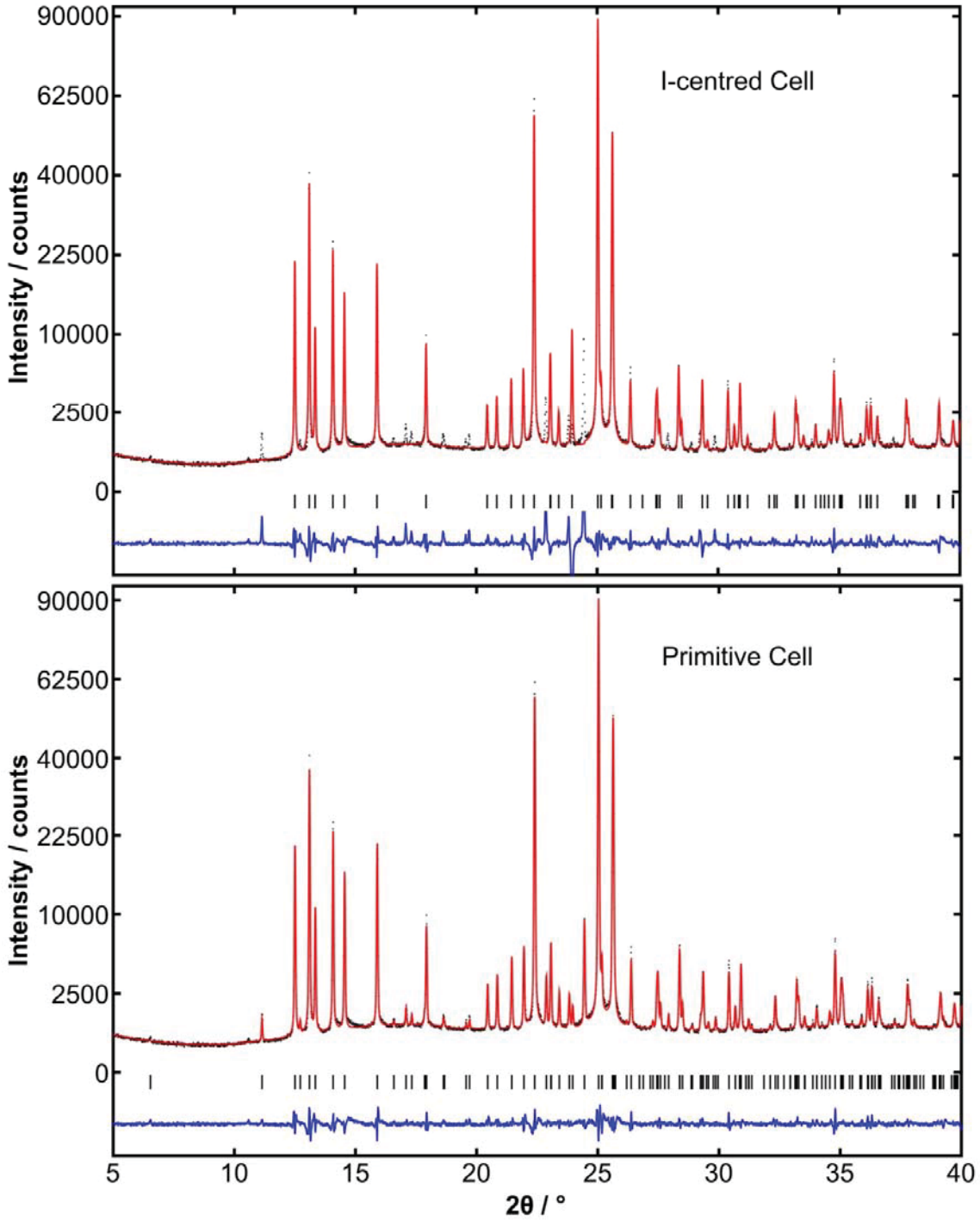

Fig. S13. LeBail fits to PXRD data of C_6F_6:C_6H_6 phase III at 215 K measured on 2.3 at the SRS with λ = 1.40302 Å. Data is shown with black dots, calculated pattern as red curve, difference between observed and calculated as blue curve, and vertical tick marks show calculated reflections positions. The plots use a square-root intensity scale to emphasise the weaker reflections. A primitive triclinic cell (*lower*) accounts for all of the observed peaks. By contrast, a body-centred triclinic cell (*upper*) with the same cell parameters accounts for only the more intense reflections e.g. the $\bar{1}02$ peak at 24.45° is not present.

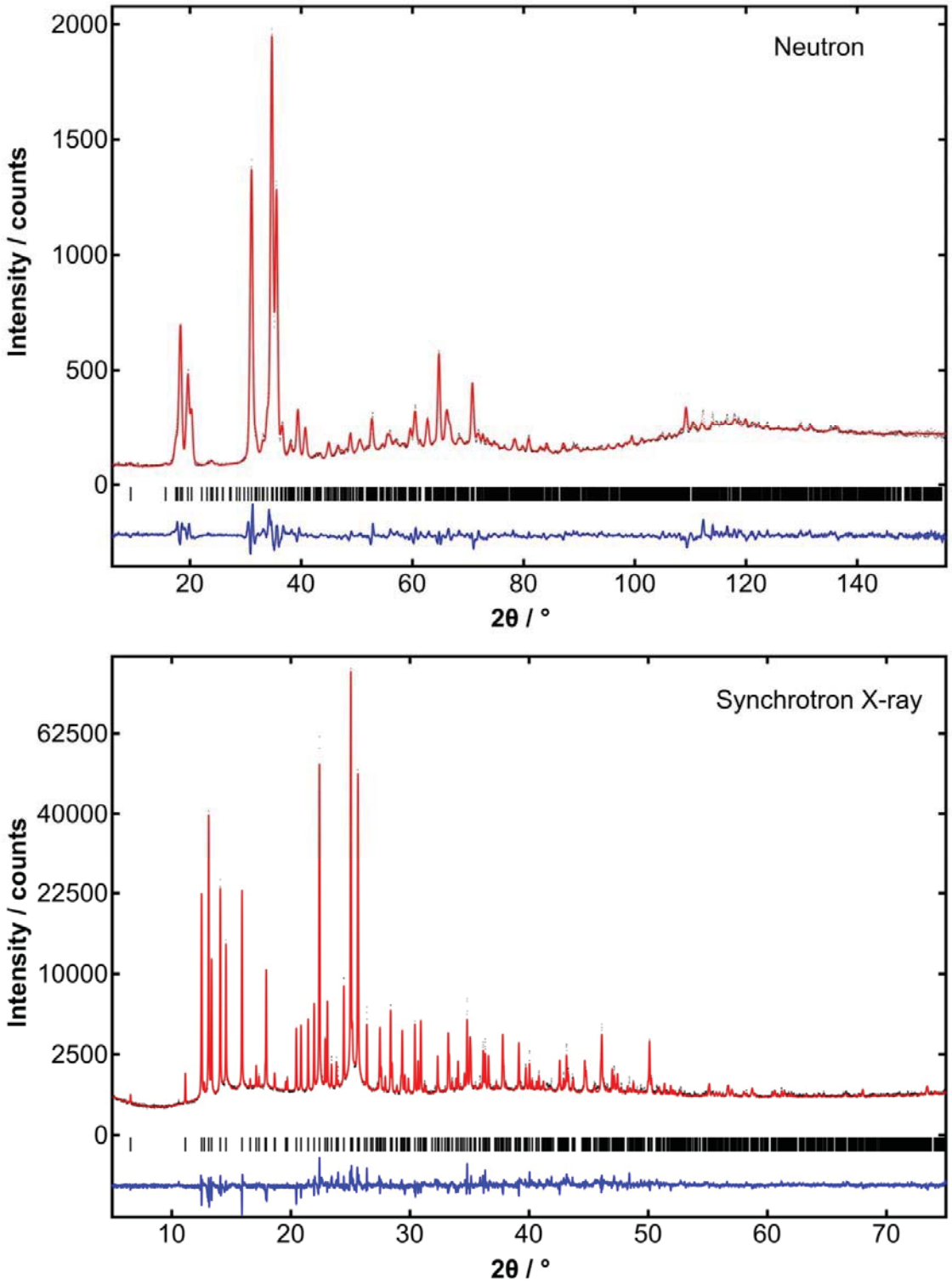

Fig. S14. Combined Rietveld refinement fit to PND data of C_6F_6:C_6D_6 phase III at 225 K (upper) and synchrotron PXRD data of C_6F_6:C_6H_6 phase III at 215 K (lower), the latter with a square-root intensity scale to emphasise the weaker reflections. Data is shown with black dots, calculated pattern as red curve, difference between observed and calculated as blue curve, and vertical tick marks show calculated reflections positions.

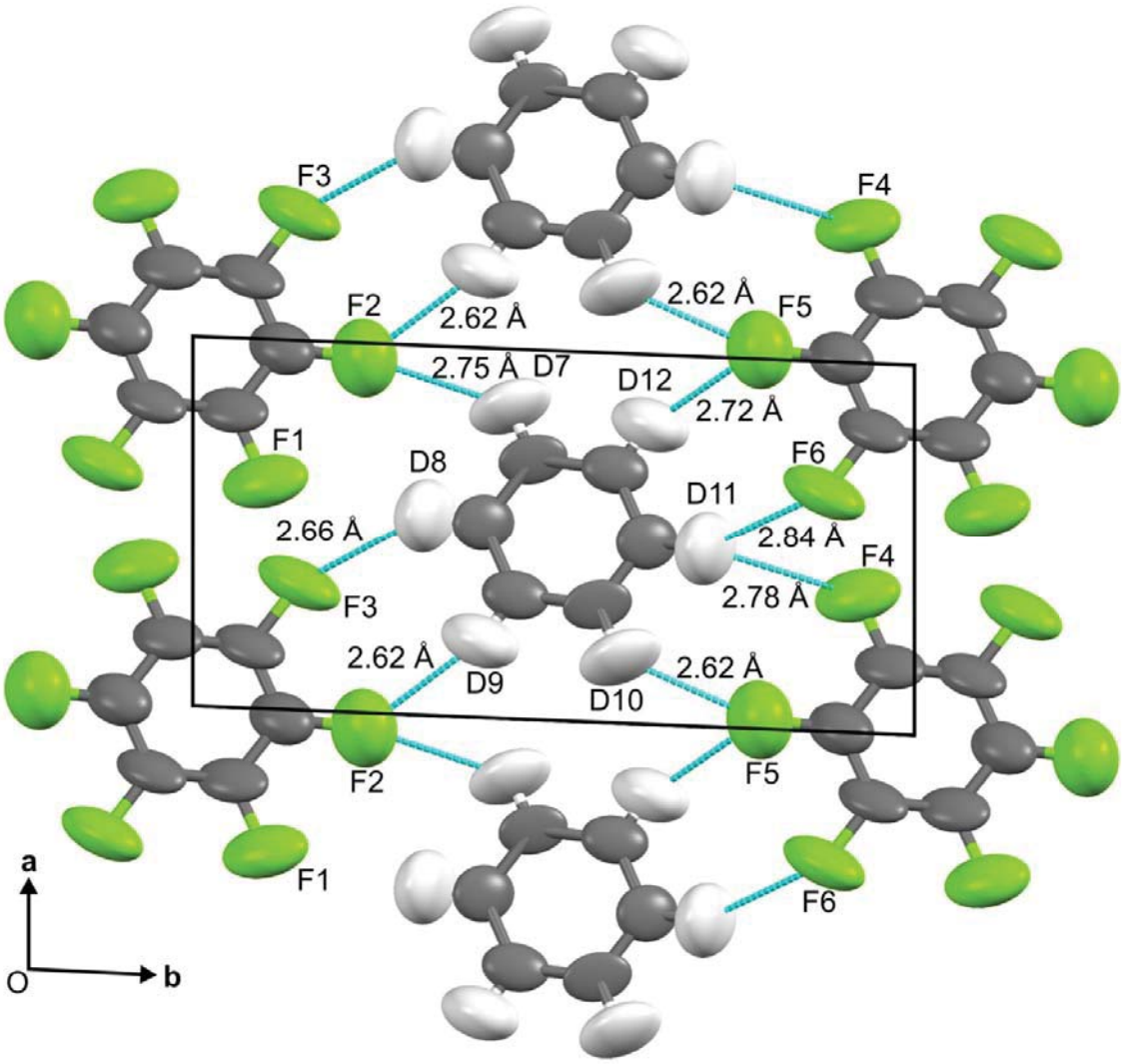

Fig. S15. Bond-dipole interactions viewed down the column axis *c* in C_6H_6:C_6F_6 phase III. Standard uncertainty on the distances shown is 0.02 Å.

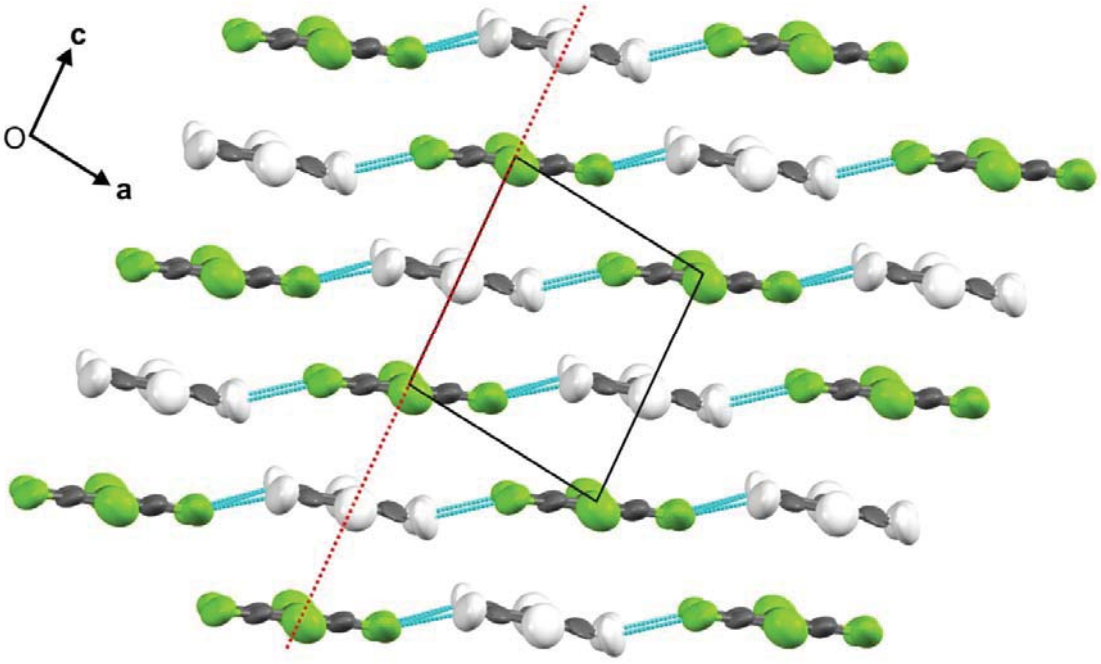

Fig. S16. Bond-dipole interactions viewed down the **b** axis in C_6H_6:C_6F_6 phase III showing sheets of molecules in addition to the columns (shown by the dotted red line) formed in all four phases by the quadrupolar interactions between the π rings of the molecules.

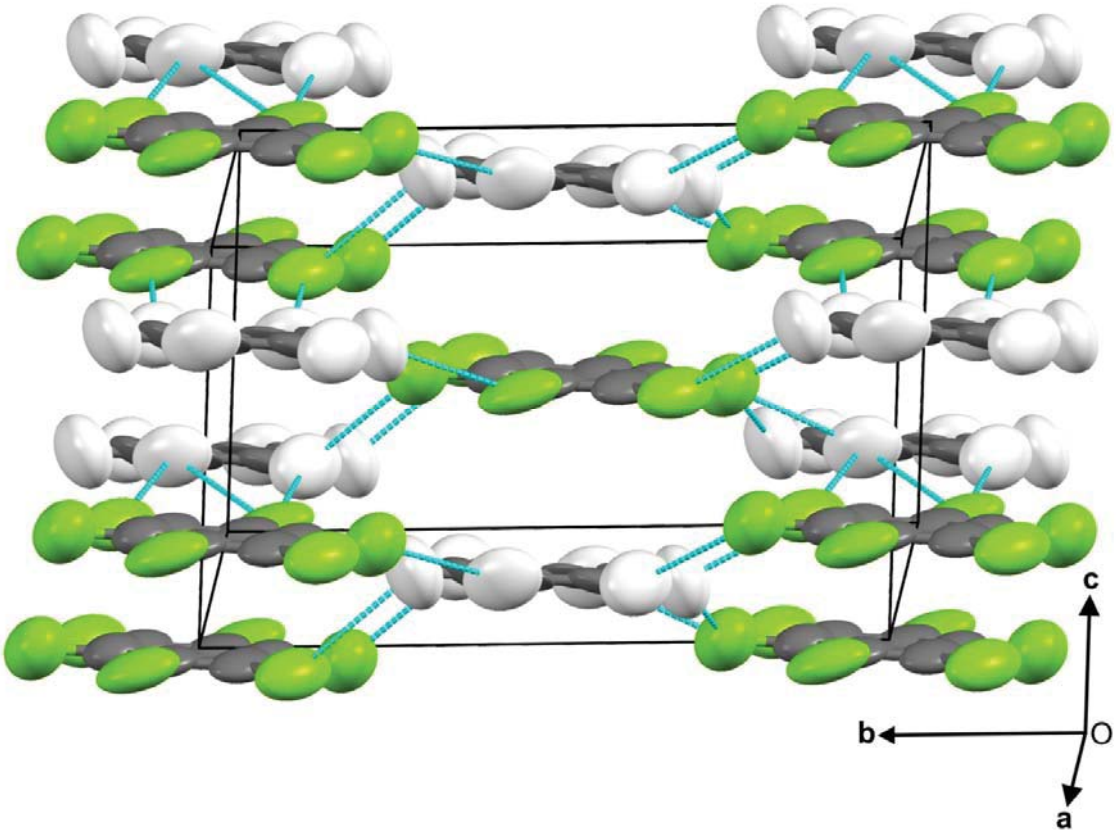

Fig. S17. Oblique view of the crystal structure of C_6H_6:C_6F_6 phase III showing additional bond-dipole interactions between layers of molecules showing the 3-D architecture.

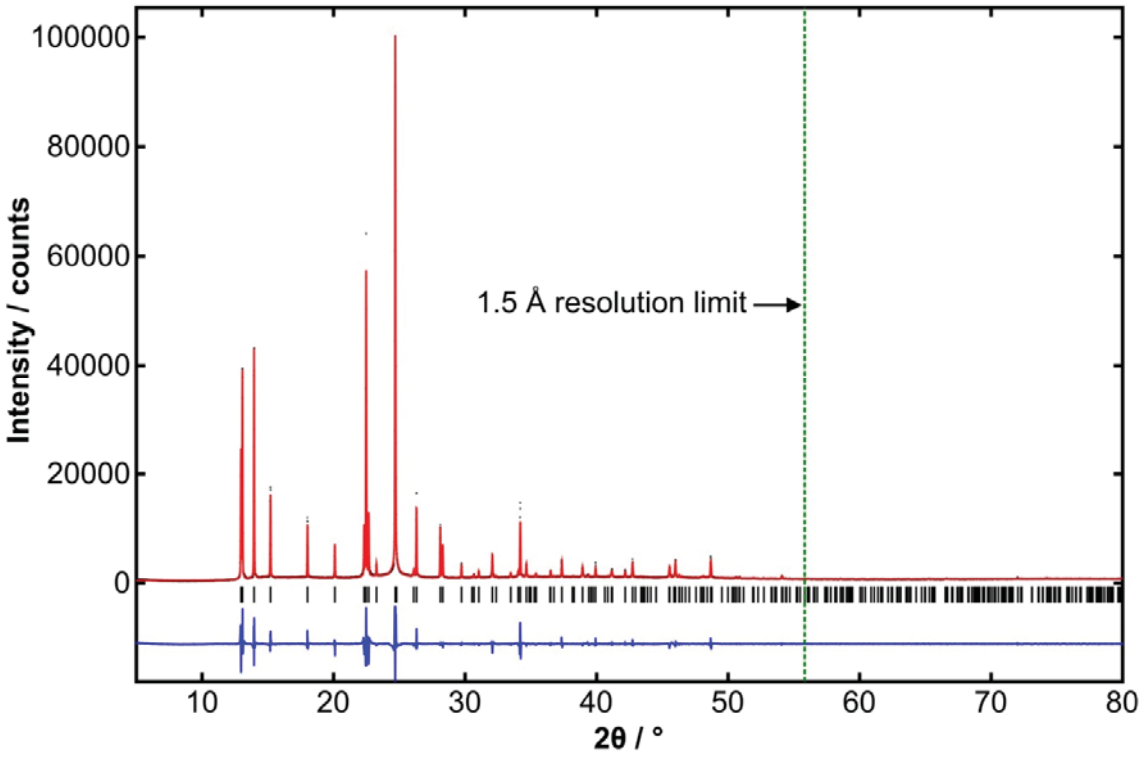

Fig. S18. LeBail fit to PXRD data of C_6F_6:C_6H_6 phase II at 260 K measured on 2.3 at the SRS with λ = 1.40302 Å. Data is shown with black dots, calculated pattern as red curve, difference between observed and calculated as blue curve, and vertical tick marks show calculated reflections positions. Sample granularity is evident for imperfections in the peak shape as random deviations from a smooth profile function are seen when individual peaks are examined in detail. There is little evidence of diffraction intensity beyond the 1.5 Å resolution limit and consequently single-crystal diffraction data for both phases I and II were not collected beyond this limit.

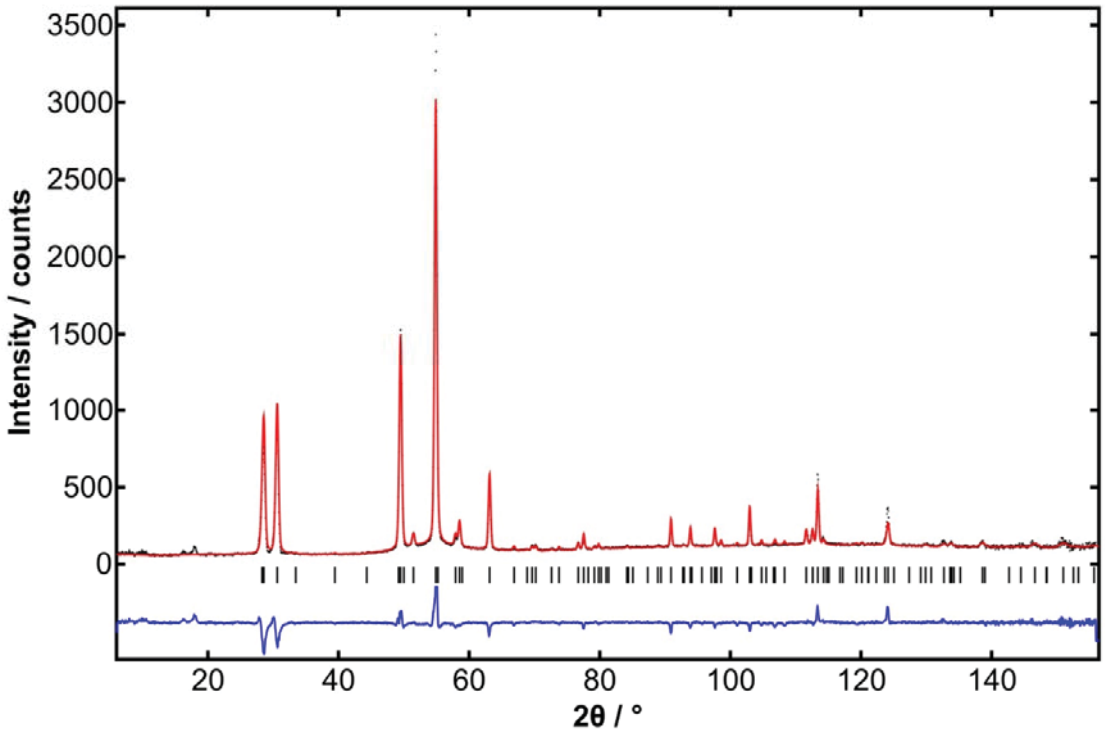

Fig. S19. Rietveld refinement fit to PND data of C_6F_6:C_6D_6 phase II at 260 K measured on D1A at the ILL with λ = 2.997 Å using the structure of phase II determined from single-crystal X-ray data. In addition to a scale factor and two peak width parameters, four lattice parameters were refined together with a single isotropic B value for the D-atoms (as for phase I). Data is shown with black dots, calculated pattern as red curve, difference between observed and calculated as blue curve, and vertical tick marks show calculated reflections positions.

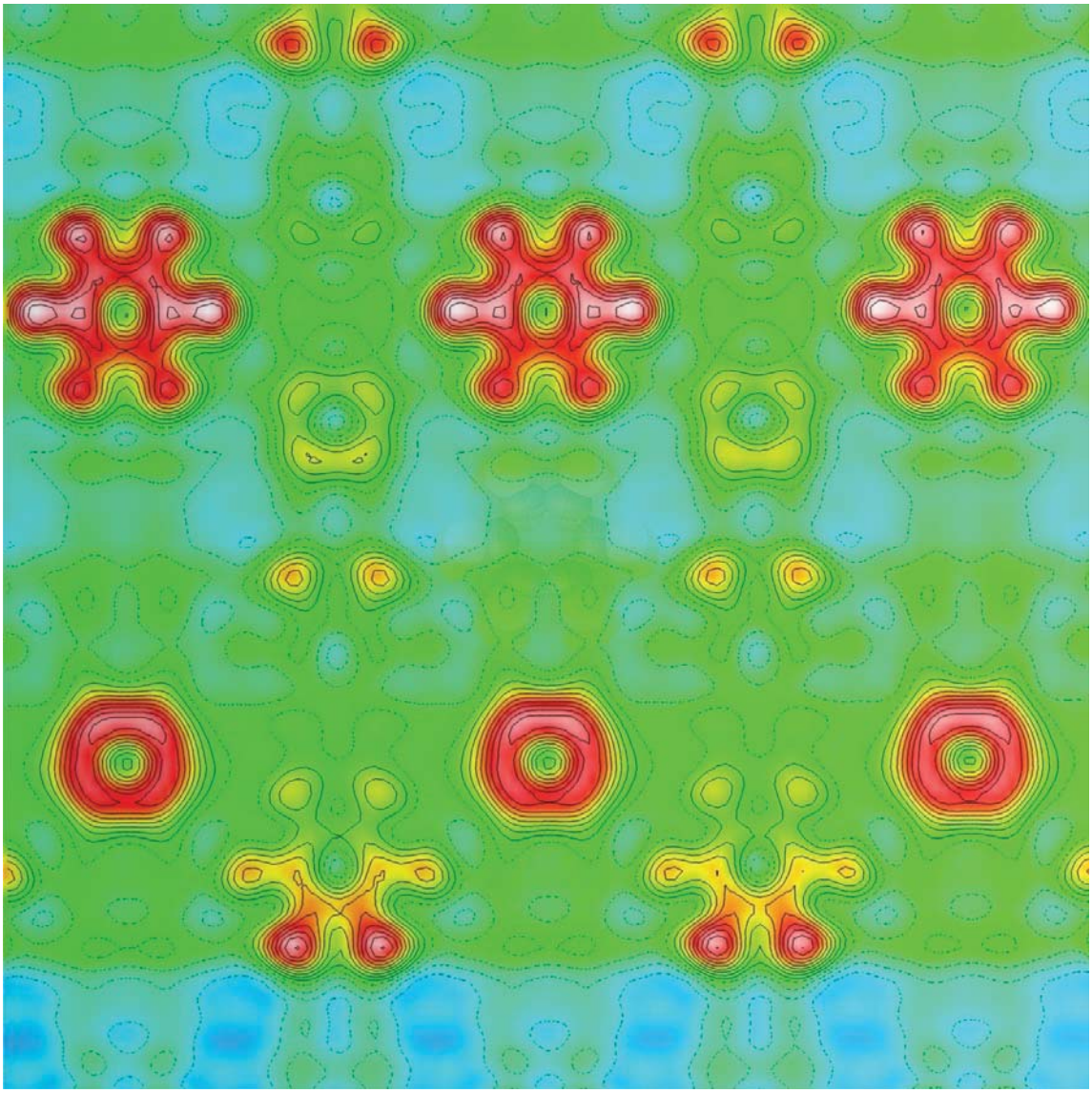

Fig. S20. Fourier map of the observed electron density of C_6H_6:C_6F_6 phase II calculated from |**F**(obs)| and phase ϕ of **F**(calc) taken across a slice of the unit cell showing the smeared out density of the C atoms of the C_6H_6 molecule due to its dynamics plus position of the C_6F_6 molecule. The motion is attributed to stochastic jump rotations about the molecular six-fold axis.

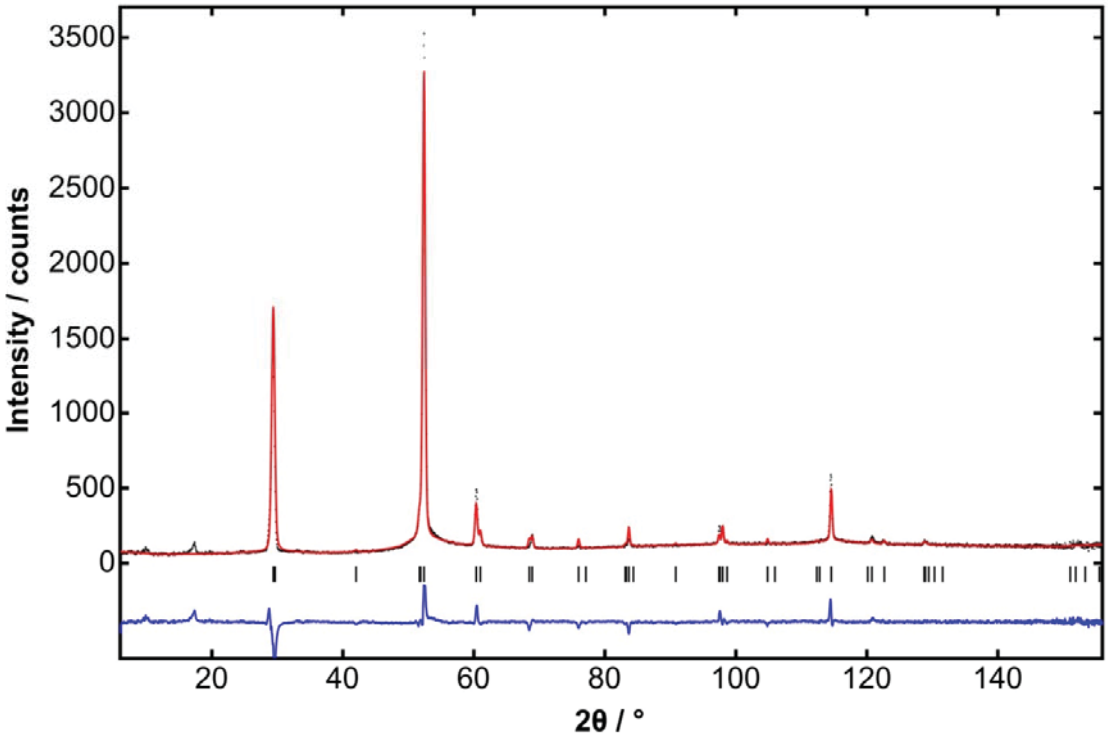

Fig. S21. Rietveld refinement fit to PND data of C_6F_6:C_6D_6 phase I at 285 K measured on D1A with λ = 2.997 Å using the structure of phase I determined from single-crystal X-ray diffraction data. Data is shown with black dots, calculated pattern as red curve, difference between observed and calculated as blue curve, and vertical tick marks show calculated reflections positions. In addition to a scale factor and peak width parameters, the two lattice parameters were refined as the sample temperature was slightly different to that of the X-ray measurement plus a single isotropic *B* value was refined for the D-atoms. The latter was required due to the higher sensitivity to the diffraction intensity of the D atoms in neutron diffraction compared to the H atoms in X-ray diffraction.

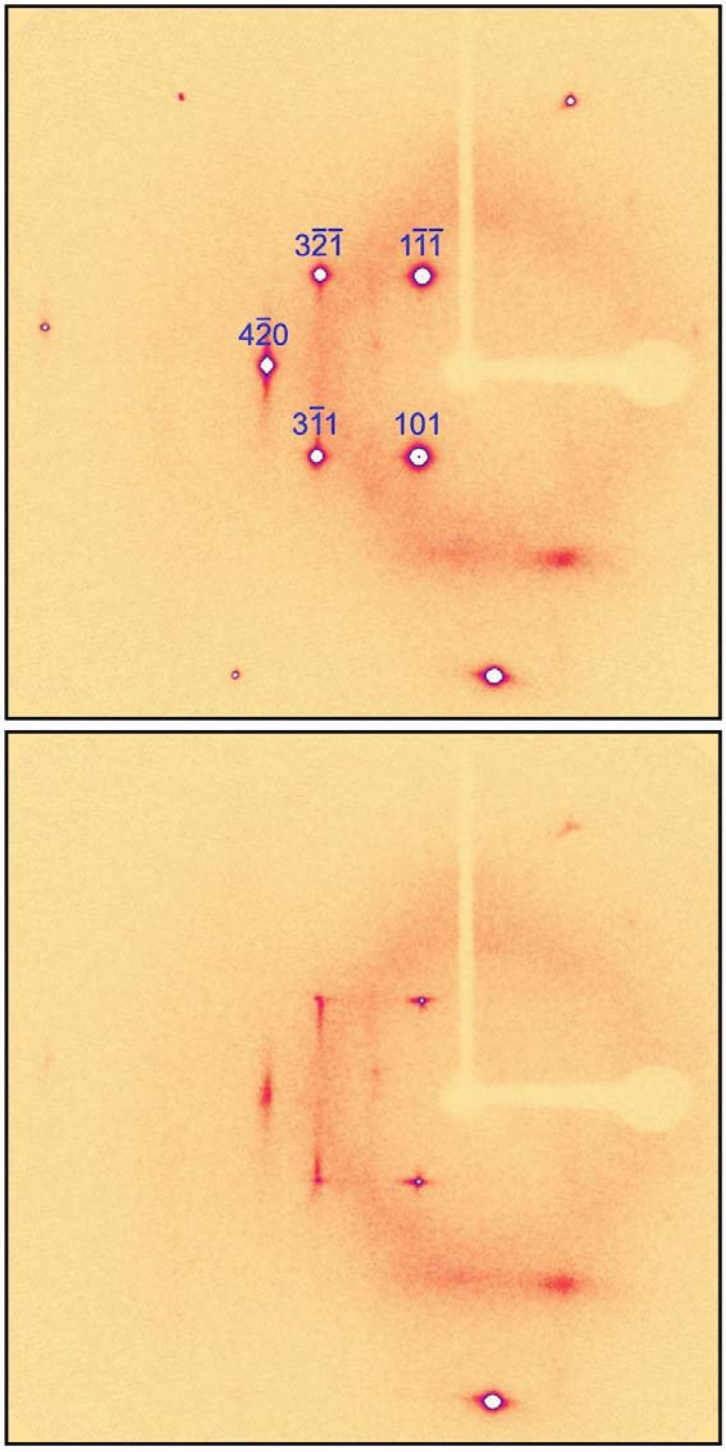

Fig. S22. Two consecutive detector frames measured on the single-crystal diffractometer of the crystal of C_6F_6:C_6D_6 in phase I showing the thermal diffuse scattering in the tails of the Bragg peaks attributed to motion of the molecules. The streaking is most pronounced along the 0kl direction for the reflections labelled above; it is visible along hk0 as well but to a lesser extent.

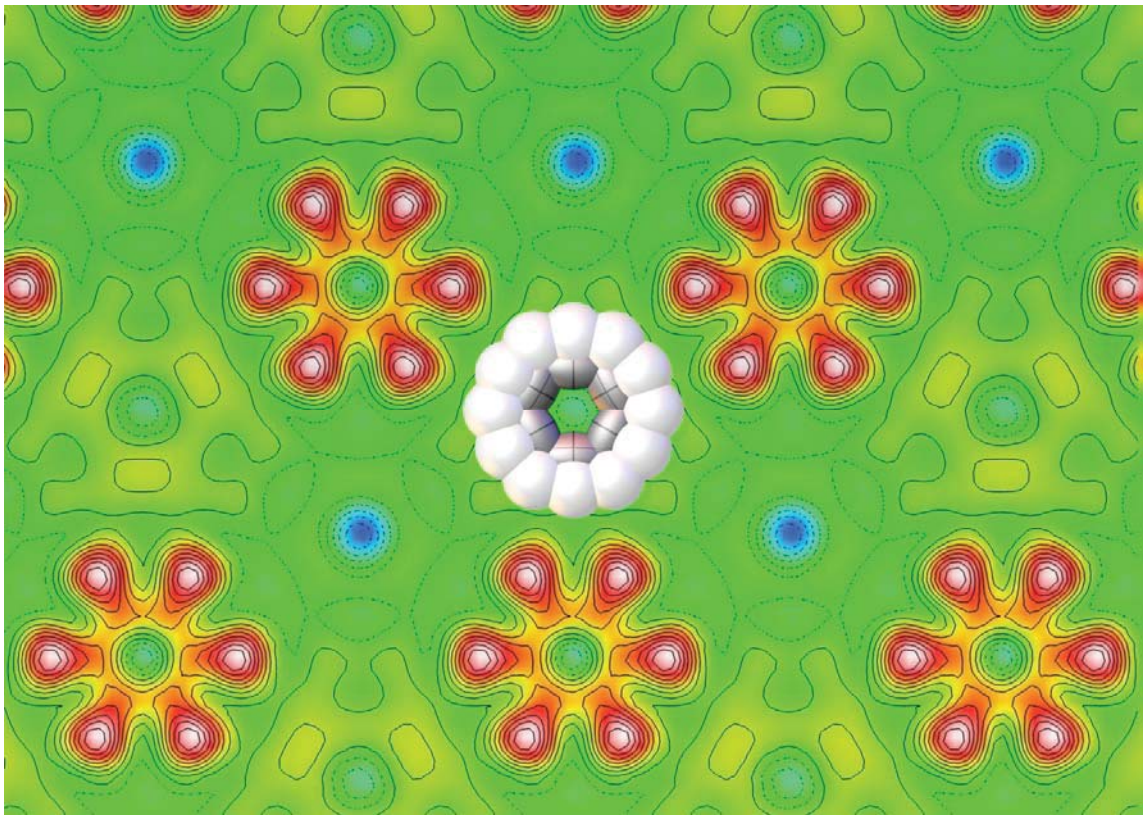

Fig. S23. Fourier map of the observed electron density of C_6H_6:C_6F_6 phase I calculated from |**F**(obs)| and phase ϕ of **F**(calc) taken across a slice of the unit cell showing distinct C_6F_6 molecules with large amplitude motion. Superimposed on the map is a representation of the motion of the atoms of a single C_6H_6 molecule (which is located above or below the plane containing the C_6F_6 rings) using ADPs shown at the 50% probability level. The Fourier map at the level at the C_6H_6 rings shows only a torus for the C atoms with the electron density of the H atoms severely delocalised. In this phase, the motion of the C_6H_6 ring is significantly closer to being a free rotor about its six-fold axis.